Dissertation

Regulation of the TCA cycle, respiration and redox balance by the gluconeogenesis enzyme PCK2 in starved lung cancer cells

submitted by

Gabriele Agnes Blümel, BSc, MSc

for the Academic Degree of

Doctor of Philosophy (PhD)

at the

Medical University of Graz

Division of Pulmonology

Department of Internal Medicine

Austria

under the Supervision of

Univ.-Ass. Priv.-Doz. Dr.med.univ. Katharina Leithner, PhD

2021

Declaration

I hereby declare that this thesis is my own original work and that I have fully acknowledged by name all of those individuals and organizations that have contributed to the research for this thesis. Due acknowledgement has been made in the text to all other material used. Throughout this thesis and in all related publications I followed the “Standards of Good Scientific Practice and Ombuds Committee at the Medical University of Graz“.

Graz, October 2021

Disclosures

Parts of this PhD thesis have been published in:

Bluemel, G.; Planque, M.; Madreiter-Sokolowski, C.T.; Haitzmann, T.; Hrzenjak, A.; Graier, W.F.; Fendt, S.-M.; Olschewski, H.; Leithner, K.; PCK2 opposes mitochondrial respiration and maintains the redox balance in starved lung cancer cells, Free Radical Biology and Medicine, 2021, 176, 34-45, https://doi.org/10.1016/j.freeradbiomed.2021.09.007 (1)

Co-authors who contributed to the publication:

Mélanie Planque
Laboratory of Cellular Metabolism and Metabolic Regulation, VIB-KU Leuven Center for Cancer Biology, VIB, Leuven, Belgium
Laboratory of Cellular Metabolism and Metabolic Regulation, Department of Oncology, KU Leuven and Leuven Cancer Institute (LKI), Leuven, Belgium

Corina T. Madreiter-Sokolowski
Gottfried Schatz Research Center for Cell Signaling, Metabolism and Aging, Molecular Biology and Biochemistry, Medical University of Graz, Graz, Austria
Energy Metabolism Laboratory, Institute of Translational Medicine, Department of Health Sciences and Technology, Swiss Federal Institute of Technology (ETH) Zurich, Zurich, Switzerland

Theresa Haitzmann
Division of Pulmonology, Department of Internal Medicine, Medical University of Graz, Graz, Austria.

Andelko Hrzenjak
Division of Pulmonology, Department of Internal Medicine, Medical University of Graz, Graz, Austria
Ludwig Boltzmann Institute for Lung Vascular Research, Graz, Austria

Wolfgang F. Graier
Gottfried Schatz Research Center for Cell Signaling, Metabolism and Aging, Molecular Biology and Biochemistry, Medical University of Graz, Graz, Austria
BioTechMed-Graz, Graz, Austria

Sarah-Maria Fendt
Laboratory of Cellular Metabolism and Metabolic Regulation, VIB-KU Leuven Center for Cancer Biology, VIB, Leuven, Belgium
Laboratory of Cellular Metabolism and Metabolic Regulation, Department of Oncology, KU Leuven and Leuven Cancer Institute (LKI), Leuven, Belgium

Horst Olschewski
Division of Pulmonology, Department of Internal Medicine, Medical University of Graz, Graz, Austria
Ludwig Boltzmann Institute for Lung Vascular Research, Graz, Austria

Katharina Leithner
Division of Pulmonology, Department of Internal Medicine, Medical University of Graz, Graz, Austria
BioTechMed-Graz, Graz, Austria

I confirm that all co-authors agreed to use their data published in Bluemel et al., 2021 (1) in my PhD thesis. As the publication has a creative commons CC-BY 4.0 attribution, the reproduction of published figures is permitted.

Please visit the following websites for permission statements:

https://s100.copyright.com/AppDispatchServlet?publisherName=ELS&contentID=S0891584921007206&orderBeanReset=true

https://creativecommons.org/licenses/by/4.0/

Additionally, I contributed to the following publications:

Grasmann, G.; Mondal, A.; Leithner, K., Flexibility and Adaptation of Cancer Cells in a Heterogenous Metabolic Microenvironment. International Journal of Molecular Sciences. 2021, 22(3)

Grasmann, G.; Smolle, E.; Olschewski, H.; Leithner, K., Gluconeogenesis in cancer cells - Repurposing of a starvation-induced metabolic pathway? Biochimica et Biophysica Acta-Reviews on Cancer, 2019, 1872(1):24-36

Leithner, K.; Triebl, A.; Trötzmüller, M.; Hinteregger, B.; Leko, P.; Wieser, B.I.; Grasmann, G.; Bertsch, A.L.; Züllig, T.; Stacher, E.; Valli, A.; Prassl, R.; Olschewski, A.; Harris, A.L.; Köfeler, H.C.; Olschewski, H.; Hrzenjak, A., The glycerol backbone of phospholipids derives from noncarbohydrate precursors in starved lung cancer cells. Proceedings of the National Acadamy of Sciences, 2018, 115(24):6225-6230

Acknowledgements

I am grateful to the PhD program Molecular Medicine (MOLMED) of the Medical University of Graz for offering excellent courses. Moreover, I want to thank the Austrian Science Fund (FWF to Katharina Leithner) for funding this project. Additionally, I was recipient of a DOC Fellowship of the Austrian Academy of Sciences.

First, I particularly want to thank my supervisor Katharina Leithner for her guidance and the great support and advice I received from her. She always had an open ear for problems I faced during the years of my PhD and she helped me to overcome them. Additionally, I want to thank Horst Olschewski for giving me the opportunity to write the thesis in the Pulmonology department.

Moreover, I want to thank my dissertation committee Horst Olschewski, Gerald Höfler and Tobias Madl for scientific guidance and Sarah Maria Fendt from KU Leuven, Belgium for welcoming me in her lab for three months. I also want to thank my fellow lab colleagues Theresa Haitzmann and Ayusi Mondal and the members of the Fendt lab for helping me with experiments, thrilling discussions and for having fun together. Additionally, I want to thank collaboration partners Mélanie Planque, Corina Madreiter-Sokolwski, Andelko Hrzenjak, Wolfgang Graier and the Core Facility of Mass Spectrometry, MedUni Graz for excellent support.

Big thanks go to all my friends and my family for having fun, doing sports, playing board games, and enjoying life together.

Especially I want to wholeheartedly thank my parents and my sister Eva. They always supported and encouraged me, and they always believed in me. This thesis would not have been possible without them.

Finally, I also want to especially thank my husband Bernhard for all the love and mental support he gave me. He was listening to all problems and cheered me up when I needed it.

Thank you!

Table of Content

Abbreviations

3PG	3-phosphoglycerate
A.U.	arbitrary units
ACTB	β-actin
ATF4	activating transcription factor 4
ATP	adenosine 5′-triphosphate
BSA	bovine serum albumin
BSO	buthionine sulfoximine
DMM	dimethyl malate
ETC	electron transport chain
$FADH_2$	flavin adenine dinucleotide
FBP	fructose-1,6-biphosphatase
FCS	fetal calf serum
GC-MS	gas chromatography-mass spectrometry
GPX	glutathione peroxidase
GSH	reduced glutathione
GSR	glutathione reductase
GSSG	oxidized glutathione
GTP	guanosine 5′-triphosphate
H_2O_2	hydrogen peroxide
HIF	hypoxia inducible factor
KEAP1	Kelch-like ECH-associated protein 1
LC-MS	liquid chromatography-mass spectrometry
MCT	monocarboxylate transporter
ME	malic enzyme
NAC	*N*-acetyl cysteine
NADH	reduced nicotinamide adenine dinucleotide
NADPH	reduced nicotinamide adenine dinucleotide phosphate

NOX	NADPH oxidases
NRF2, *NFE2L2*	nuclear factor erythroid 2-related factor 2
NSCLC	non-small cell lung cancer
$O_2^{\cdot -}$	superoxide anion
OAA	oxaloacetate
OH·	hydroxyl radical
OXPHOS	oxidative phosphorylation
PC	pyruvate carboxylase
PCK1	cytoplasmic isoform of phosphoenolpyruvate carboxykinase
PCK2	mitochondrial isoform of phosphoenolpyruvate carboxykinase
PDH	pyruvate dehydrogenase
PDK1	pyruvate dehydrogenase kinase 1
PEP	phosphoenolpyruvate
PEPCK	phosphoenolpyruvate carboxykinase
PK	pyruvate kinase
PKM2	M2 isoform of pyruvate kinase
PPP	pentose phosphate pathway
PRDX	peroxiredoxins
ROS	reactive oxygen species
RT-qPCR	quantitative real-time PCR
SCLC	small cell lung cancer
shRNA	short hairpin RNA
siRNA	small interfering RNA
SOD	superoxide dismutase
TCA cycle	tricarboxylic acid cycle
TXN	thioredoxin
TXNRD	TXN reductase
UCP2	uncoupling protein 2

Zusammenfassung

Tumorzellen sind infolge ihres hohen Verbrauchs und unzureichender Versorgung häufig mit wechselnden Nährstoffkonzentration und Mangel konfrontiert. Dadurch sind Anpassungen des Stoffwechsels erforderlich. Gluconeogenese, in großen Teilen die Umkehrung der Glykolyse, ist ein Stoffwechselweg der durch Mangel aktiviert wird. Das Hauptenzym, welches Gluconeogenese initiiert, ist das Enzym Phosphoenolpyruvate-Carboxykinase (PEPCK, PCK). Es ermöglicht die Verstoffwechselung von Oxalacetat, einem Tricarbonsäure (TCA) Zyklus (Krebszyklus) Zwischenprodukt zu Phosphoenolpyruvat. PCK2 (PEPCK-M). Die mitochondriale Isoform von PEPCK wird in Tumoren, unter anderem in Lungenkrebs, exprimiert. Die Expression ist vorteilhaft für das Tumorwachstum in diversen *in vitro* und *in vivo* Modellen und ermöglicht die Biosynthese von Gluconeogenesesprodukten in Krebszellen bei Glucosemangel.

In dieser Arbeit wird gezeigt, dass in zwei verschiedenen Lungenkrebs Zelllinien unter Glucose und Serummangel, PCK2 Hemmung zu erhöhtem Vorkommen und Umwandlung von TCA Zyklus Produkten führte. Dieser Effekt wurde durch PCK2 Re-expression aufgehoben. Glucose- und Serummangel induzierten mitochondriale Atmung welche zusätzlich durch PCK2 Hemmung erhöht war. Mitochondriale Atmung induziert oxidativen Stress. PCK2 beeinflusste das Vorkommen von Superoxid und H_2O_2 nicht, jedoch war Glutathionoxidation durch PCK2 Hemmung vermehrt. Außerdem führte PCK2 Hemmung zu verschlechterter Kolonienbildung bei Behandlung mit Nährstoffmangelmedium, dem konnte durch die Zugabe von Antioxidantien entgegengewirkt werden. Diese Ergebnisse konnten durch die Zugabe des TCA Zyklus Zwischenprodukts Dimethylmalat reproduziert werden und konnten somit mit der durch Hemmung von PCK2 hervorgerufenen Aktivitätssteigerung des TCA Zyklus verknüpft werden.

Zusammenfassend, limitiert die kataplerotische Aktivität von PCK2 bei Glucose- und Serummangel die mitochondriale Atmung und hält das Glutathion Redox Equilibrium aufrecht. In dieser Arbeit wird die Rolle der Gluconeogenese in der Anpassung von Tumorzellen an Nährstoffmangel erforscht und es wird gezeigt, dass PCK2 Expression durch Atmung induzierten oxidativen Stress limitiert.

Abstract

Cancer cells often face starvation and fluctuating nutrient concentration, due to inadequate supply and high consumption, requiring metabolic adaptions. Gluconeogenesis, largely the inverse pathway of glycolysis, is a metabolic pathway activated by starvation. The key enzyme, initiating gluconeogenesis is phosphoenolpyruvate carboxykinase (PEPCK, PCK) which converts the tricarboxylic acid (TCA) cycle (Krebs cycle) metabolite oxaloacetate to the glycolytic intermediate phosphoenolpyruvate. The mitochondrial isoform of PEPCK, PCK2 (PEPCK-M), is expressed by different tumors, including lung cancer. Expression of PCK2 has been shown to enhance tumorigenesis in diverse *in vitro* and *in vivo* models and enables the synthesis of gluconeogenic products in glucose starved cancer cells.

In this thesis, it was identified that in two different lung cancer cell lines the amount and the interconversion of TCA cycle metabolites were enhanced by PCK2 silencing upon treatment with glucose and serum starvation media. This effect was reversed by PCK2 re-expression. Upon treatment with glucose and serum starvation media, the mitochondrial respiration was increased in comparison to nutrient replete conditions, and it was additionally augmented by PCK2 silencing. Mitochondrial respiration induces oxidative stress. Superoxide and H_2O_2 levels were not affected but glutathione oxidation was increased by PCK2 inhibition. Furthermore, PCK2 silencing significantly impaired colony formation upon starvation treatment, and was rescued by addition of antioxidants. Importantly, these findings could be linked to the enhancement of TCA cycle activity by PCK2 silencing, as the effects were phenocopied by supplementing media with the TCA cycle intermediate dimethylmalate.

In summary, the cataplerotic activity of PCK2 limits mitochondrial respiration and balances the glutathione redox equilibrium upon glucose and serum starvation. In this thesis, gluconeogenesis, as an adaptive response of tumor cells to nutrient starvation is examined and the role of PCK2 expression to limit respiration-induced oxidative stress is identified.

1. Introduction

1.1. Lung cancer

Lung cancer is the most common newly diagnosed tumor worldwide and leads to the highest tumor-related mortality (2,3). The major cause of lung cancer is smoking, but also exposure to radon or asbestos, air pollution or passive smoking lead to an enhanced predisposition (2,4). Based on histology, lung cancer is classified into two different sub-types, non-small cell lung cancer (NSCLC) and small cell lung cancer (SCLC) accounting for 85% and 15% of newly diagnosed lung cancer cases respectively (3). Diagnosis often occurs at an advanced stage (3,5), leading to a poor survival rate (3,6). Due to late diagnosis the five-year survival over all patients is 15%, however for patients diagnosed with stage I NSCLC tumors five-year survival can reach 55-77% (6).

Depending on the tumor stage, treatment consists of surgery, which is only possible if diagnosis occurs at an early stage, and radiotherapy often in combination with chemotherapy. Since almost two decades targeted therapies can be offered to NSCLC patients with specific mutations. Epidermal growth factor receptor mutations or translocations of the anaplastic lymphoma kinase gene or the tyrosine-protein kinase ROS1, occur in around 15%, 5% and 1% of patients respectively (7). These are driver mutations that are specifically treatable and therefore have a better prognosis, however these mutations are relatively rare (3,8). More than half of NSCLC tumors are driven by unknown oncogenic driver mutations not allowing targeted therapies (8). Recently developed immune therapies with checkpoint-kinase inhibitors showed dramatic and durable responses in a subset of NSCLC patients, however this type of treatment is limited to a small proportion of cases (7,9). As treatment options are currently limited to patients with a certain mutational background and the overall survival rate is poor, it is necessary to identify alternative treatment opportunities. The metabolic adaptation of NSCLC is extensively studied, to identify potential vulnerabilities that can potentially be exploited as alternative treatment approaches through the utilization of metabolic inhibitors (10).

1.2. Cancer metabolism

In the presence of oxygen (O_2), differentiated cells convert glucose to pyruvate in a series of reactions (Figure 1, left panel). This process is termed glycolysis and results in the net production of 2 molecules adenosine 5′-triphosphate (ATP) and 2 molecules nicotinamide adenine dinucleotide (NADH) per molecule glucose (11,12). Pyruvate is then metabolized to acetyl-Coenzyme A (acetyl-CoA), which then condensates with oxaloacetate (OAA). This leads to the formation of citrate and fueling of the tricarboxylic acid (TCA) cycle (citric acid cycle, Krebs cycle). In a series of reactions, one complete round through the TCA cycle results in the complete oxidation of acetyl-CoA and the reformation of OAA and yields CO_2, H_2O, and the reducing equivalents NADH and flavin adenine dinucleotide ($FADH_2$) (11,12). During oxidative phosphorylation (OXPHOS), NADH and $FADH_2$ are oxidized in the electron transport chain (ETC) in the mitochondrion. O_2 is reduced to H_2O and the forward flux of electrons through the four complexes of the electron transport chain leads to the generation of a proton gradient over the inner mitochondrial membrane. When protons are flowing back through the fifth complex, the ATP synthase, ATP is formed (11,12). As the process of mitochondrial respiration is highly efficient, aerobic glycolysis accounts for a total production of up to 36 mol ATP per mol glucose, summing up ATP derived from glycolysis and through oxidative phosphorylation (11,12).

However, if oxygen is limited, cells perform anaerobic glycolysis as they cannot rely on mitochondrial respiration (Figure 1, middle panel) (11). They metabolize glucose to pyruvate and instead of fueling pyruvate into the TCA cycle, lactic acid is formed. Through the formation of lactic acid, NADH is regenerated, and glycolysis can persist. This leads to the production of 2 mol ATP per mol glucose and lactic acid secretion. As the ATP generation is low, anaerobic glycolysis is not favorable for differentiated cells (11).

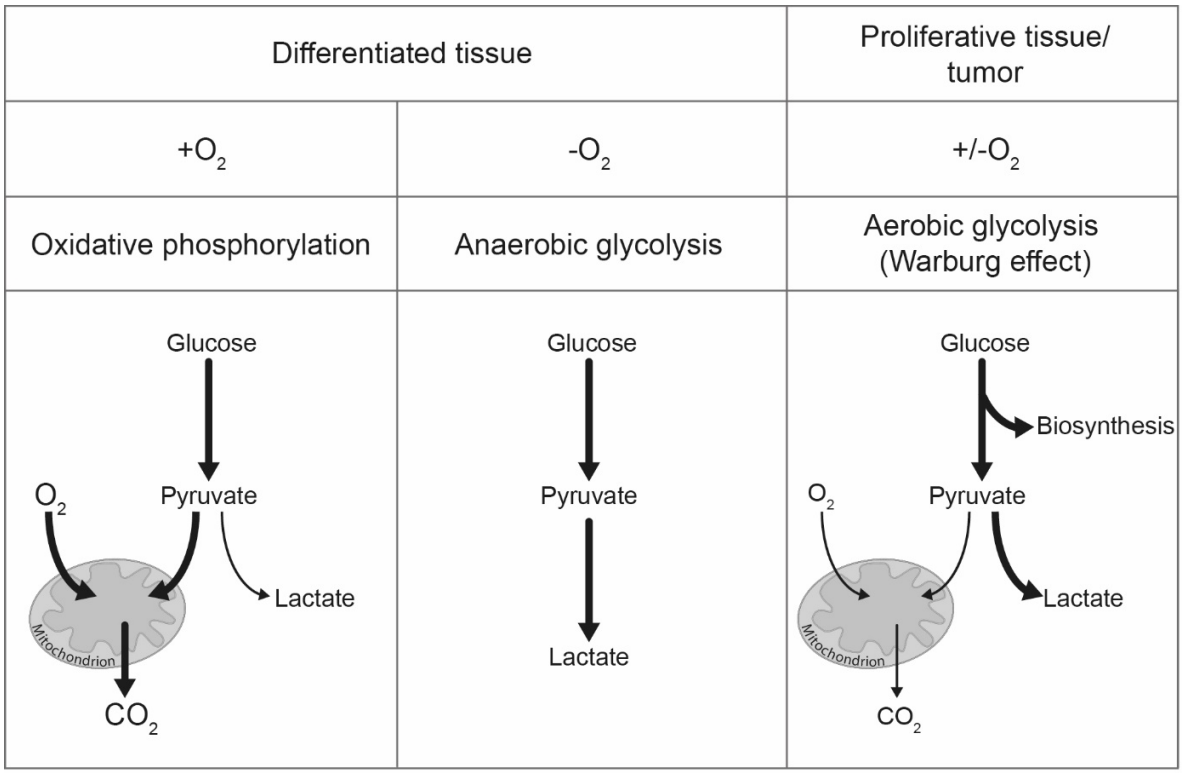

Figure 1: Different metabolic pathways of glucose, depending on oxygen availability and between differentiated tissue and proliferating cells. If O_2 is present most differentiated cells fully oxidize glucose. Lactic acid production is minimized, and pyruvate is metabolized to acetyl-CoA which is completely oxidized in the TCA cycle. This results in the production of NADH and $FADH_2$ which are oxidized during oxidative phosphorylation yielding a high amount of ATP. If O_2 availability is limited, differentiated cells perform anaerobic glycolysis, leading to the formation of lactic acid and yielding a low amount of ATP. In fast proliferating cells and tumor cells mainly rely on aerobic glycolysis, a phenotype defined as "Warburg effect". Despite the presence of O_2, glycolysis is highly enhanced and mitochondrial respiration is relatively reduced. Glycolytic intermediates are shunted into biosynthetic pathways and pyruvate is primarily metabolized into lactic acid.

Proliferative cells and many cancer cells almost exclusively rely on aerobic glycolysis, although oxygen is available and the TCA cycle and OXPHOS remain functional (11,13) (Figure 1, right panel). Metabolic reprogramming which includes altering of the energy metabolism is considered as one hallmark of cancer cells (14). Tumors limit the entering of pyruvate derived from glycolysis into the TCA cycle and therefore also the amount of mitochondrial respiration (11,14). Already in the 1920s Otto H. Warburg described that cancer cells show a high glucose consumption leading to lactic acid secretion (15), this phenomenon is called Warburg effect. The high glucose consumption by tumors is also used for detection and staging of tumors with ^{18}F-desoxyglucose positron emission tomography (FDG-PET) (16). Regarding ATP and therefore energy generation, aerobic glycolysis is less efficient than oxidative phosphorylation

(11,14). However, if cells face high glucose supply, they benefit, as they gain different crucial building blocks such as nucleotides, lipids, and carbohydrates necessary for fast growth and proliferation. One pathway, highly upregulated by tumor cells is the pentose phosphate pathway (PPP) which leads to the formation of ribose and the reducing equivalent nicotinamide adenine dinucleotide phosphate (NADPH) (11,17). However, if glucose availability is low, tumor cells are forced to switch their energy metabolism back to mitochondrial respiration, which was shown to be augmented upon glucose deprivation in many different cancer cell lines (18).

The Warburg effect implies that cancer cells limit entering of glucose derived acetyl-CoA into the TCA cycle. This favors shunting of glycolytic intermediates into the formation of biosynthetic intermediates. Cancer cells therefore alter the activity of enzymes, mediating terminal steps of the glycolytic pathway. First, they reduce the rate of pyruvate formation from phosphoenolpyruvate (PEP) at the step of pyruvate kinase (PK). PK exists in two splice variants, and proliferating cells preferentially express PKM2. Upon high glucose availability PKM2 is dimeric instead of tetrameric due to tyrosine phosphorylation and therefore has a low activity (12). Moreover, acetylation and reactive oxygen species (ROS) induced oxidation limit PKM2 activity (12). Additionally, the activity of pyruvate dehydrogenase (PDH), located in the mitochondrial matrix, which mediates acetyl-CoA formation from pyruvate, is reduced (19). PDH activity is inhibited through abundant NADH and ATP availability and it is inactivated through phosphorylation by the enzyme pyruvate dehydrogenase kinase 1 (PDK1) (12), whose expression is regulated by c-myc or β-catenin signaling (19). Due to inhibition of PDH, pyruvate is converted into lactic acid and exported to the tumor microenvironment, instead of entering the TCA cycle. Enhanced lactic acid export leads to extracellular acidification, which promotes angiogenesis, metastasis formation and increased invasiveness (20,21). Acidosis in the tumor microenvironment alters immune cell function, including suppression of T-cell proliferation and cytokine production, along with effects directly mediated by lactate, such as histone lactylation (20,22).

A constant supply with nutrients, especially glucose and oxygen are essential for cancer growth. Therefore, tumors induce angiogenesis, the de-novo formation of vessels, at an early stage of tumor formation (14). However, newly synthesized vessels are often leaky and compressed and oxygen and nutrient availability is frequently not sufficient (23). Inadequate angiogenesis in combination with high consumption of glucose, result in a nutrient poor tumor

microenvironment and heterogeneous tumor areas with varying metabolite concentrations (23). This results in nutrient and oxygen gradients, correlating with increasing distances to the vessels (24) (Figure 2). Recently, in a murine pancreatic cancer model, nutrient availability was discovered to differ between the plasma and the tumor interstitial fluid. Whereas glucose levels in the tumor microenvironment were on average only half the levels of plasma, the glutamine concentration was comparable (25).

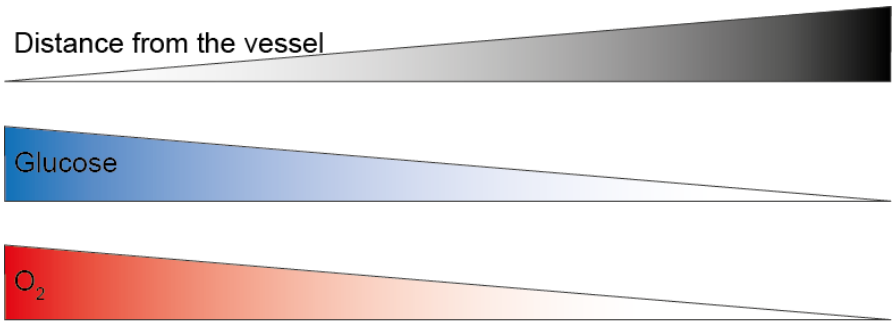

Figure 2: Distance to the vessels influences the nutrient availability for cancer cells. An increasing distance to the vessel correlates with reduced oxygen and glucose availability (24).

Varying nutrient compositions and starvation conditions force cancer cells to alter their metabolism to secure survival and growth (13,26). In numerous studies it has been shown that cancer cells thrive in different nutritional niches and interact with stroma cells, fibroblasts or other surrounding cells resulting in a complex rewiring of metabolism to meet the cancer cells´ demands (27,28). These adaptive processes are particularly important during invasion and metastasis. Metabolic flexibility and plasticity, meaning the flexible utilization of alternative metabolites and processing substrates through different pathways respectively, is a critical determinant of cancer progression and metabolic flexibility is connected to increased tumor aggressiveness (28).

If glucose availability is limited, cancer cells show a high metabolic flexibility and utilize various alternative metabolites for anabolism (reviewed in (29)). Surprisingly, irrespective of the prominent role of glucose and its huge consumption by cancer cells, cellular mass is in major parts amino acid derived (30). The most prominent fuel, beside glucose, is glutamine (31), although its role seems to be more relevant in *in vitro* systems compared to *in vivo* models (32). Glutamine serves as an anaplerotic metabolite as it fuels the TCA cycle through a conversion

to glutamate and further to α-ketoglutarate. By contributing to the TCA cycle and to pyruvate and acetyl-CoA formation from TCA cycle anions it is also a respiratory fuel. Additionally, glutamine serves as nitrogen donor for nucleotides and non-essential amino acids (Figure 3, blue boxes). Further, it is involved in the cellular antioxidant defense via glutathione (GSH), a tripeptide consisting out of glutamate, cysteine, and glycine. Glutamine is the direct precursor of glutamate, which is not only directly contributing to GSH but also exported by the antiporter system xCT, also referred to as SLC7A11, to import cystine, which is then processed intracellularly to cysteine, also necessary for GSH biosynthesis (31). Another compound serving as metabolic fuel of cancer cells is lactic acid, although it is generally considered as a waste product, as it is often exported by cancer cells. In glucose deprived media but also in a rat model bearing human breast cancer upon the presence of glucose, lactic acid has been shown to be taken up and to be metabolized by tumor cells (33). Lactic acid is taken up via the monocarboxylate transporter (MCT) and is metabolized to pyruvate and fuels the TCA cycle as first shown in cervix squamous cell carcinoma cancer cells (34). Additionally, many other metabolites such as pyruvate, alanine, acetate, and free fatty acids were shown to be imported by cancer cells and to support metabolic flexibility (reviewed in (13,29,35)).

The TCA cycle is a central biosynthetic hub. It connects mitochondrial respiration, glycolysis, and anabolic biosynthetic pathways (12). Nutrients such as glutamine or lactic acid can feed into the TCA cycle and enter different biosynthetic pathways e.g., amino acid, nucleotide or fatty acid synthesis (Figure 3, blue boxes). Additionally, as NADH and $FADH_2$ are yielded via cycling of metabolites through the TCA cycle, also mitochondrial respiration is fueled. For continued TCA cycle flux, anaplerosis, the fueling of the TCA cycle and cataplerosis, the removal of TCA cycle metabolites, need to be balanced (36).

1.3. Gluconeogenesis

Gluconeogenesis is in large parts the reverse pathway of glycolysis. It describes the *de novo* formation of glucose or glycolytic biosynthetic intermediates from non-carbohydrate compounds such as lactate or amino acids such as alanine or glutamine. Complete gluconeogenesis only occurs in classical gluconeogenic tissues as liver and kidney, due to the lack of glucose-6-phosphatase in other tissues. Most glycolytic enzymes react bidirectional, in the direction of glycolysis and gluconeogenesis. However, the steps from glucose to glucose-6-phosphate, fructose 6-phosphate to fructose 1,6-bisphosphate as well as from PEP to pyruvate are irreversible. For gluconeogenesis the reverse reactions are catalyzed by glucose-6-phosphatase, fructose-1,6-bisphosphatase (FBP) and phosphoenolpyruvate carboxykinase (PEPCK), respectively (Figure 3, orange arrows). PEPCK not directly mediates the backward direction but catalyzes the guanosine triphosphate (GTP) dependent reaction from OAA to PEP. PEPCK therefore initializes gluconeogenesis and all other branching biosynthetic pathways from small carbon substrates (Figure 3, orange boxes) e.g., nucleotides (ribose-5-phosphate), serine, glycine and lipids (glycerol-3-phosphate). In the latter case, gluconeogenesis does not yield glucose and this process is sometimes referred to as “abbreviated” or “partial” gluconeogenesis. Two isoforms of PEPCK are known, the cytoplasmic form PCK1 (PEPCK-C), is present in classical gluconeogenic tissues such as the liver, kidney, and the intestine (reviewed in (37)) and PCK2 (PEPCK-M), the mitochondrial isoform. PCK2 is more broadly expressed and in addition to gluconeogenic tissue it has been also found in other tissues, including the lung (38,39).

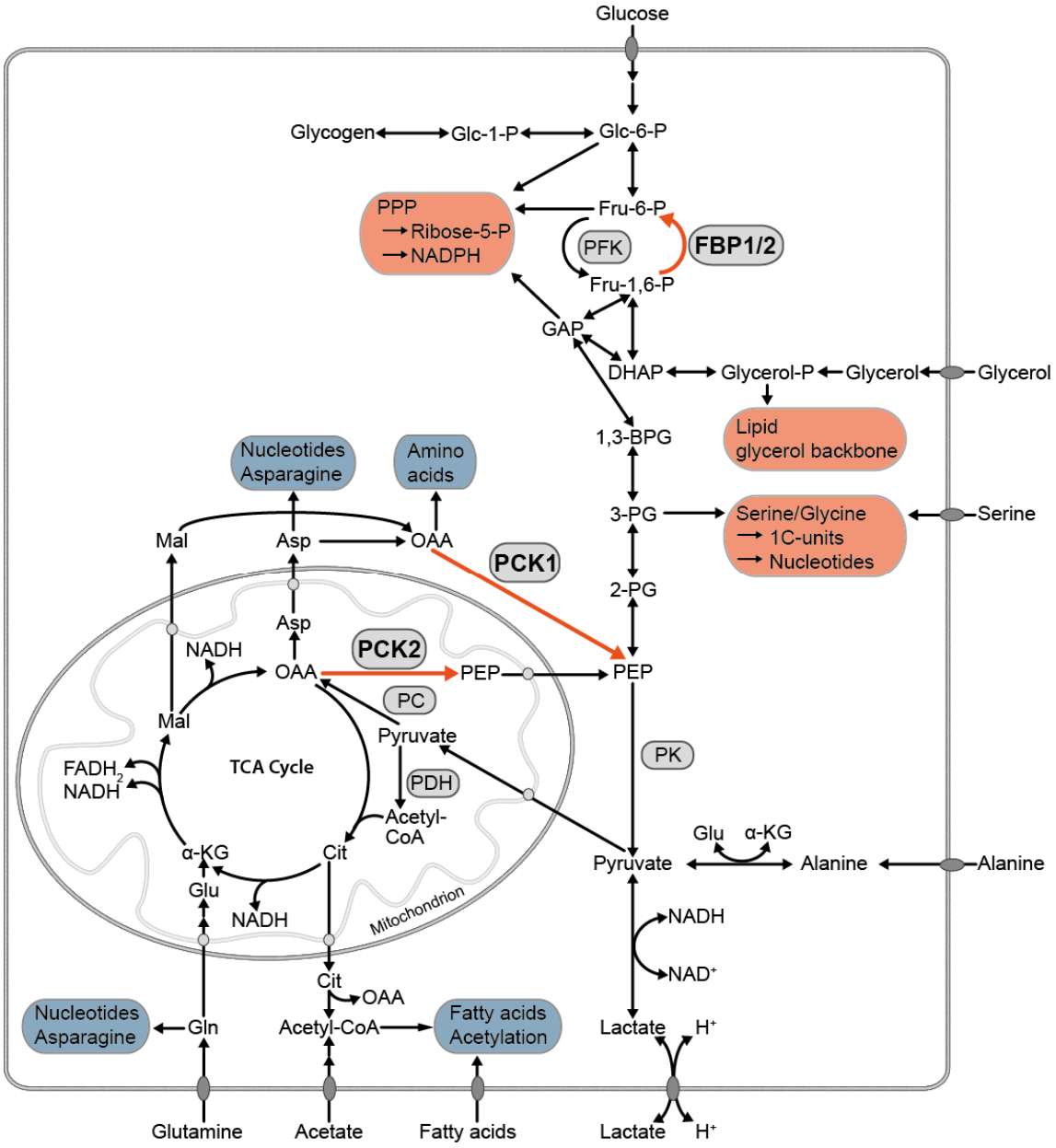

Figure 3: Scheme of the glycolytic and the gluconeogenic pathways and the flexible utilization of various nutrients. Depending on the nutritional state of the cancer cell, either glucose or non-carbohydrate compounds such as glutamine, acetate, lactic acid, alanine, or also fatty acids can be utilized to fuel anabolism. The glycolytic pathway is mostly bidirectional. Reactions that need to be by-passed by phosphoenolpyruvate carboxykinase (PCK1/PCK2) and by fructose-1,6-bisphosphatase (FBP1/2) are shown with orange arrows. Upon glucose deprivation PCK1 and PCK2 mediate the synthesis of glycolytic biosynthetic intermediates via partial gluconeogenesis (shown in orange boxes). Biosynthetic intermediates not derived via gluconeogenesis are shown in blue boxes. PPP, pentose phosphate pathway; PFK, phosphofructokinase; PK, pyruvate kinase; PC, pyruvate carboxylase; PDH, pyruvate dehydrogenase; TCA, tricarboxylic acid cycle; OAA, oxaloacetate; PEP, phosphoenolpyruvate. The figure is reproduced with modifications with permission from the authors and the publisher from (37).

Recently, the contribution of the gluconeogenic precursors lactate, alanine, glycerol, and glutamine to complete and partial gluconeogenesis was quantified in mice. In fasted mice, 40% of the plasma glucose is 13-C lactic acid derived, whereas glycerol accounted for 33%, and alanine and glutamine for 10% each, after 2.5 hours infusion (40). Interestingly, gluconeogenesis contributed significantly to the glycolytic pools in addition to glycolysis and to local glycogen breakdown (40). Such a partial gluconeogenesis was discovered in gluconeogenic tissues but also in lung, heart, brain and other peripheral tissues. The biggest contributor to gluconeogenesis derived glycolytic intermediates was lactic acid. In the lung around 25% of the 3-phosphoglycerate (3-PG) pool was lactic acid derived after 2.5 hours of infusion with 13-C lactic acid. The contribution of gluconeogenesis to glycolytic pools was higher in fasting animals than in the fed state (40).

Already in 2014, Leithner et al. showed that lactic acid derived gluconeogenesis, mediated by PCK2, is exploited by lung cancer cells grown in glucose and serum starved media and enables cancer cell survival and proliferation upon nutrient shortage. Since then, PCK2 was shown to be expressed and have pro-proliferative effects in different tumor models, including lung, breast, and prostate cancer (41-46). PCK1 expression was identified to support tumor growth in tumor models including colon cancer (47,48). In tumor repopulating cells of melanoma PCK2 expression was found to be downregulated and its overexpression impairs tumorigenicity (49), however in the same model, the PCK1 expression was shown to be enhanced and it had pro-proliferative effects (48). Whereas PEPCK expression has mainly tumor promoting effects in tumors not originating from classical gluconeogenic tissues, in liver and kidney cancer, PEPCK expression was downregulated and its expression inhibits cancer growth (reviewed in (37)). Upon treatment with low glucose media, PCK1 or PCK2 overexpression reduced liver cancer survival due to an induced energy crisis (50).

Multiple biosynthetic pathways, branching from glycolysis were discovered to be fueled by partial gluconeogenesis via PCK2 or PCK1, especially under nutrient deprivation. Stable isotope-resolved metabolomics revealed that lactic acid and glutamine serve as gluconeogenic precursors in cancer cells (41,43,44,47,51,52). Upon glucose depletion, PCK2 was shown to mediate the biosynthesis of serine and glycine (43,51,52). In a lung cancer cell line, around 40% of total serine levels were shown to be supplied by glutamine in a PCK2 dependent manner after 48 hours of treatment in the absence of glucose. The same study revealed that

additionally around 12% of the purine nucleotide ATP are glutamine derived and therefore of gluconeogenic origin (43). In lung cancer cells upon glucose and serum starvation but not under nutrient replete conditions, both lactic acid and glutamine were incorporated into the glycerol backbone of phospholipids. Furthermore, it was shown that PCK2 expression maintains the levels of the glycerophospholipid phosphatidylethanolamine (44). In PCK1 expressing colon cancer cells, gluconeogenesis derived ribose biosynthesis was discovered, and its abundance was enhanced upon reduced glucose supplementation (47).

To ensure a flexible response to the cellular nutritional state and resulting metabolic needs, expression of PCK1 and PCK2 is tightly regulated. In classic gluconeogenic tissues the presence of glucagon and glucocorticoids induces PCK1 expression whereas the presence of insulin represses it (described and reviewed in detail in (53)). Additionally, PCK2 and partly also PCK1 appear to be regulated by different metabolic cues and nutrient sensing pathways, as was intensively studied in recent years in cancer cells. PCK2 expression has been shown to be upregulated upon glucose or amino acid starvation and endoplasmatic reticulum (ER) stress (41-44). Amino acid deprivation and ER stress, induced by the unfolded protein response, upregulate activating transcription factor 4 (ATF4) that has a binding site in the PCK2 promotor (42). The activity of PCK2 is influenced by mitochondrial concentrations of GTP, likely formed by succinyl-CoA synthetase (SUCLG2), a TCA cycle enzyme. SUCLG2 is upregulated by glucose deprivation, in contrast to the ATP producing form of succinyl-CoA (SUCLA2) (43). Silencing of the GTP producing form leads to reduced cell survival, whereas the ATP producing isoform shows no effect (43). Under normoxia, simultaneous silencing of hypoxia inducible factor (HIF1 and HIF2) inhibited low glucose induced PCK2 protein expression (43), however upon hypoxia, conditions that lead to HIF stabilization, PCK2 protein levels were found to be decreased (39). Nitric oxide, produced by the arginine-citrulline cycle, was shown to lead to S-nitrosylation of PCK2 in cancer cells grown in glucose deprived media and this post-translational modification increased gluconeogenesis from glutamine (51). Moreover, MondoA, a nutrient-sensing transcription factor belonging to the MYC superfamily, was shown to induce PCK2 expression (54). Additionally, purine element binding protein α has a binding motif in the PCK2 promotor resulting in enhanced expression (55). Post-translational modifications of PCK1, acetylation and sumolyation, both were shown to increase degradation of PCK1 (56,57). Interestingly the effect of the tumor suppressor p53 and the protein complex mTOR Complex 2 (mTORC2) that regulates cell survival and proliferation, on the expression of PCK1 and PCK2

was shown to be depending on the tissue where the tumor arises from. Expression of p53 increased PCK2 expression in the liver cancer cell line HepG2 (58) whereas it decreased PCK1 expression in different cancer cell lines and in mouse liver (59). mTORC2 led to the downregulation of PCK1 in cancer cells derived from classic gluconeogenic tissues but not in tumor cells from other tissues (60).

The pro- or antitumorigenic role of PCK2 in cancer progression, appears to be highly context dependent and is reviewed in (37). In lung cancer, PCK2 expression has pro-survival and pro-proliferative effects under glucose starvation conditions, and its expression supports xenograft growth *in vivo* (41,43,44). In addition to mediating anabolic biosynthetic functions, PCK1 or PCK2 are directly involved in removing TCA cycle anions (cataplerosis). PCK2 expression in tumor cells has been shown to decrease the amount of TCA cycle metabolites in tumor initiating cells of prostate cancer and melanoma and in breast cancer cells upon hypoxia (45,49,61). Contrary, PCK2 silencing decreased the levels of TCA cycle metabolites in HeLa cells in a re-expression reversible manner under high glucose conditions (52). However, the role of PCK2 on the TCA cycle and on the mitochondrial respiration under starvation has not been addressed so far.

1.4. Reactive oxygen species

Reactive oxygen species (ROS) describe a group of molecules that are by-products from the cellular oxygen metabolism, and that have a higher reactivity than molecular oxygen. Intracellularly, ROS are originating from mitochondrial respiration, NADPH oxidases, or as by-product during protein folding in the ER (12,62) (Figure 4). Low levels of ROS are reversible and pro-tumorigenic (63). In the nucleus, ROS can induce DNA mutagenesis and tumor initiation. In tumor progression mild ROS levels induce activation of signaling pathways and transcription factors inducing metabolic and antioxidative adaptations that promote tumorigenesis (13,63). However, as high ROS levels lead to damage and cell death, cancer cells need to control their ROS levels and upregulate antioxidant defense mechanisms.

Mitochondrial respiration is the major cause of reactive oxygen species (ROS) as 1-2% of oxygen utilized by mitochondria is converted to superoxide anion ($O_2^{\cdot -}$) (64,65). Superoxide is quickly converted to hydrogen peroxide (H_2O_2), either by superoxide dismutase (SOD) or non-enzymatically (Figure 4). H_2O_2, a membrane permeable, non-radical ROS, might also be a by-product of protein folding in the ER (62). H_2O_2 is membrane permeable. At low levels (up to 10 nM) it serves as an important signaling molecule (63). In the Fenton reaction, H_2O_2, which has a low reactivity, reacts with metal cations (Fe^{2+} or Cu^{+}) and a highly reactive hydroxyl radical ($OH\cdot$) is formed. To avoid the generation of harmful $OH\cdot$, cells rapidly dismutate H_2O_2 to water by catalase, peroxiredoxins or by glutathione peroxidases (Figure 4). Thereby in peroxiredoxins an intersubunit dissulifde bond is generated. Glutathione peroxidases use GSH as co-factor, which is oxidized to GSSG. Dissulfide bonds of peroxiredoxins are regenerated by thioredoxin (TXN), a protein antioxidant. Oxidized TXN and GSSG are subsequently reduced by TXN reductase (TXNRD) or by glutathione reductase (GSR), both reducing NADPH (63) (Figure 4). If $OH\cdot$ is not scavenged it might react with polyunsaturated fatty acids and initiate lipid peroxidation. Lipid radicals are formed, which react with further polyunsaturated fatty acids, propagating the peroxidation process (63) (Figure 4). At high levels lipid peroxidation initiates ferroptosis, a type of cell death that relies on iron (63). Glutathione peroxidase 4 (GPX4) buffers lipid peroxidation and prevents ferroptosis at the expense of reduced GSH (66).

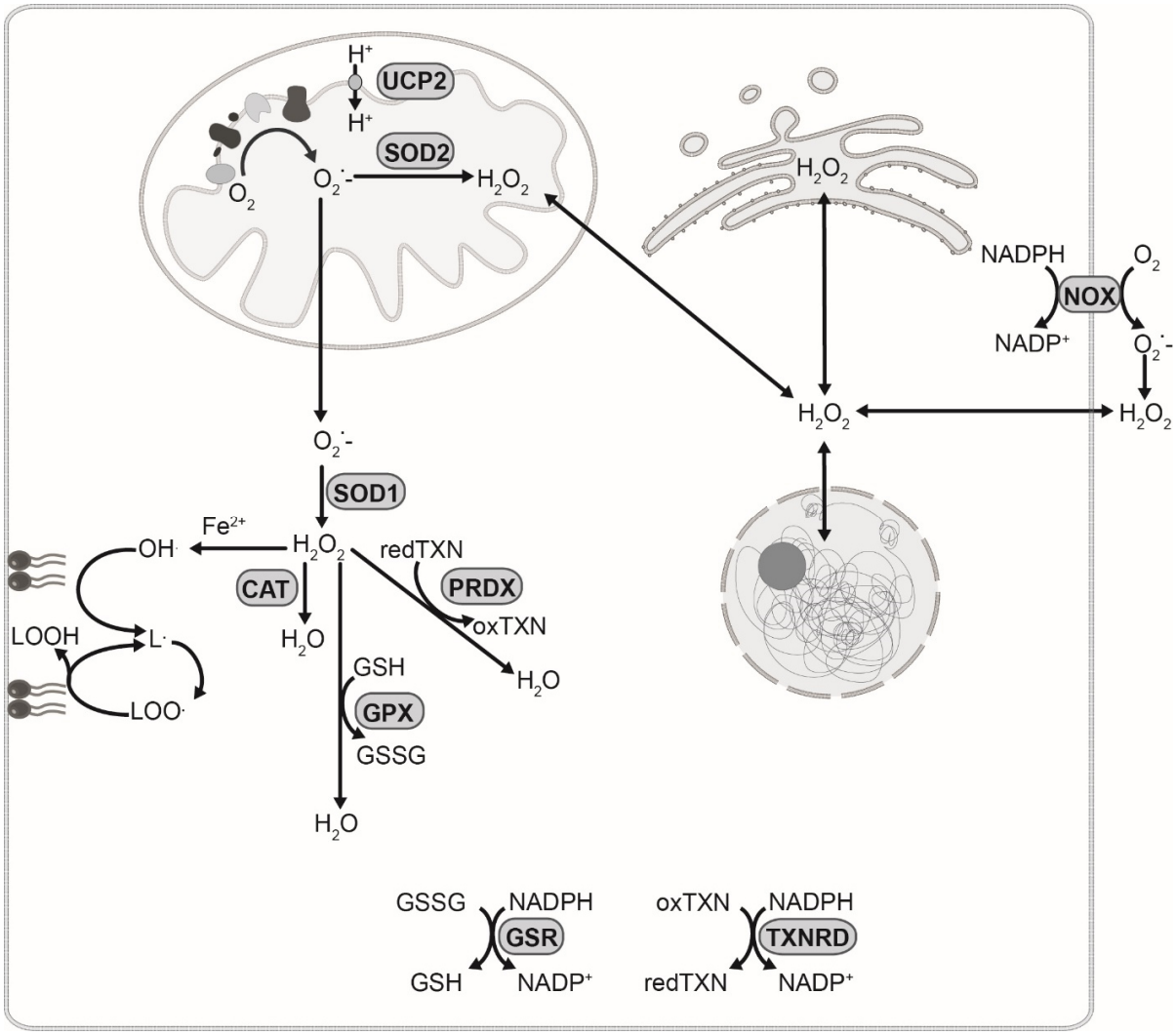

Figure 4: The origin, interconversion, and neutralization of reactive oxygen species (ROS). Major sources of ROS are the electron transport chain, protein folding in the ER and NADPH oxidases (NOX). Superoxide ($O_2^{\cdot-}$) is produced either by respiration or by NOX. The production of mitochondrial $O_2^{\cdot-}$ can be reduced by uncoupling protein 2 (UCP2), as the enzyme transports protons over the mitochondrial membrane which reduces the membrane potential and therefore $O_2^{\cdot-}$ production. Additionally, $O_2^{\cdot-}$ is quickly converted to hydrogen peroxide (H_2O_2) by superoxide dismutase (SOD1, SOD2) or non-enzymatically. H_2O_2 may mediate mutagenesis but it is also important for cellular signaling. It is rapidly neutralized to H_2O by catalase, glutathione peroxidase (GPX), having glutathione as a co-factor or peroxiredoxins (PRDX), with thioredoxin (TXN) as a co-factor. Oxidized glutathione and thioredoxin might be reduced by glutathione reductase (GSR) and TXN reductase (TXNRD) at the expense of NADPH. If H_2O_2 reacts with Fe^{2+} a hydroxyl radical ($OH\cdot$) is formed. It can react with polyunsaturated fatty acids and start the self-perpetuating process of lipid peroxidation.

Compared to non-proliferating cells, cancer cells have higher local ROS levels (13). Therefore, they increase cellular antioxidative capabilities to maintain their redox equilibrium. One transcription factor, detrimental for the upregulation of antioxidative pathways is nuclear factor erythroid 2-related factor 2 (NRF2, encoded by *NFE2L2*). In non-cancerous cells NRF2 interacts with Kelch-like ECH-associated protein 1 (KEAP1), leading to proteasomal degradation of NRF2 (12,13). ROS modify cysteine residues of KEAP1, which then leads to the dissociation and therefore to the accumulation of NRF2. NRF2 upregulates the transcription of various genes in the TXN and GSH dependent antioxidative pathways (13,63,67,68). Increased NRF2 levels are observed in many different cancer types. They result from mutations in KEAP1 or NRF2, increased NRF2 expression or reduced expression of KEAP1, all leading to NRF2 accumulation (63).

Additionally, cells utilize uncoupling proteins (UCP), commonly known from brown adipose tissue for thermogenesis, for antioxidant defense. Especially UCP2 has been described to be hijacked by cancer cells to enable proton uncoupling, meaning that protons can cross the inner mitochondrial membrane along the gradient to the matrix in a controlled manner, but uncoupled to the ATP synthase (64,69) (Figure 4). By decreasing the membrane potential through proton uncoupling, less superoxide is produced, however also the ATP yield of mitochondrial respiration is decreased (64,69). In different cancer types, UCP2 expression was found to be upregulated and connected to tumor progression (64). Moreover, adenine nucleotide translocase (ANT), catalyzing ATP/ADP exchange over the mitochondrial membrane, shows uncoupling activity, which is induced by superoxide levels (70).

To avoid cell death through elevated ROS levels, cancer cells have an enhanced demand in NADPH and GSH. Boosted glycolysis, as discussed before, results in enhanced fueling of glucose into the PPP to ensure adequate NADPH supply (71). GSH is highly present in tumor tissue in different cancer types in comparison to normal tissue (68). It can be either restored from GSSG at the expense of NADPH or de-novo synthesized from glycine, cysteine and glutamate, as described before (68). The most limiting amino acid is cysteine, however different cancer cells upregulate the glutamate-cystine antiporter SLC7A11, a NRF2 target (72). Cystine imported via SLC7A11 is then reduced to cysteine in order to generate GSH.

Especially under glucose deprivation cancer cells need accurate balancing of redox levels and a high capability of antioxidant defense pathways. On the one hand mitochondrial respiration is increased (18), due to energy requirements leading to enhanced production of ROS. On the other hand, NADPH/NADP levels are reduced (73) as glucose derived NADPH production is reduced (13). This results in enhanced cytotoxicity of glucose deprived cells due to ROS (73). While the literature on antioxidant defense in cancer cells is growing, very few is known about the role of antioxidant responses under starvation conditions that may be associated with enhanced mitochondrial respiration and thus ROS burden.

1.5. Hypothesis

Anaplerosis, the fueling of the TCA cycle, and cataplerosis, the removal of TCA cycle metabolites, need to be balanced to maintain a continued flux (36). The abundance of OAA and acetyl-CoA are detrimental for the regulation of the TCA cycle which is not only an important biosynthetic hub, but additionally generates reducing equivalents necessary for mitochondrial respiration (12,74). Under nutrient replete conditions, mediators of the TCA cycle and mitochondrial respiration have been well studied (19). Upon glucose deprivation, mitochondrial respiration is enhanced in different cancer cell lines (18), however, not much is known about the regulation of the TCA cycle under starvation.

It remains to be clarified, if the expression of the cataplerotic enzyme PCK2, playing an essential role for tumor growth in *in vitro* and in *in vivo* studies, has an impact on the regulation of the TCA cycle upon glucose starvation. Previous studies addressed the PCK2 dependent abundance of TCA cycle intermediates and mitochondrial respiration under nutrient replete conditions (45,46,49,52,61). However, upon nutrient starvation, conditions often present intratumorally that have been shown to increase PCK2 expression and activity (41-44), the abundance of TCA cycle intermediates has not been studied yet. Altered TCA cycle flux might subsequently influence mitochondrial respiration and therefore the cellular redox balance. This study might help to understand the effects of PCK2 on tumor survival under nutrient starvation conditions additionally to its role for biosynthesis of gluconeogenic intermediates.

2. Methods

2.1. **Cell lines**

The human NSCLC cell lines NCI-H23 (H23) and A549 were obtained from American Type Culture Collection (ATCC, Manassas, VA, USA) and Cell Lines Service (Eppelheim, Germany) respectively. H23 cells were maintained in RPMI 1640 cell culture media (Gibco, Waltham, MA, USA), A549 cells were maintained in DMEM/F-12 (Gibco). Both growth media were complemented with glutamine and antibiotics (both Gibco) and 10% fetal calf serum (FCS, Biowest, Nuaillé, France). For maintenance, passaging occurred twice per week. For experiments, if not otherwise stated, 22,000 cells/cm^2 were seeded in growth media. Treatment occurred 20-24 hours after plating. To this end, cells were rinsed two times with phosphate buffered saline (PBS, PAN-Biotech, Aidenbach, Germany) and incubated either with non-starvation (nstv) or starvation (stv) media. Treatment media were prepared by supplementing glucose and glutamine free RPMI SILAC medium or glucose and glutamine free DMEM (both Gibco) with 10 or 0.2 mM (non-starvation/starvation) glucose (Sigma Aldrich, Waltham, MA, USA), 0% or 10% dialyzed FCS (Thermo Scientific, Waltham, MA, USA), 2 mM glutamine (Sigma Aldrich) and antibiotics. RPMI SILAC treatment media additionally contained 1.15 mM arginine and 0.27 mM lysine (both Sigma Aldrich). Mycoplasma tests were performed regularly. Short Tandem Repeat (STR) analysis forcell line confirmation was performed using the PowerPlex 16HS System (Promega, Madison, WI) for both cell lines by the Core Facility Alternative Biomodels and Preclinical Imaging, Medical University of Graz.

2.2. **Stable expression of PCK2 shRNA**

H23 cells, stably transfected with commercially available non-silencing control shRNA (ctrl sh) or PCK2 shRNA (Qiagen, Hilden, Germany) were previously generated, selected for two weeks with 1 µg/µL puromycin (Sigma Aldrich) and monoclonal subcultures from PCK2 shRNA and control shRNA were created and kindly provided by K. Leithner (44). Cells were maintained with media containing 0.5 µg/µL puromycin which was absent throughout experiments. Specificity of PCK2 shRNA mediated effects was confirmed by transfecting PCK2 silenced cells with a shRNA resistant PCK2 cDNA plasmid. The shRNA binding site was mutated at three codons (Eurofins Genomics, Ebersberg, Germany), without any alterations in the amino acid sequence and cloned into a pCMV6-AC expression vector (Origene, Rockville, MD). As a

control the empty expression vector was utilized. Transfection was performed with 0.5-1 µg cDNA/200,000 cells using the jetPRIME transfection reagent (Polyplus, Illkirch, France).

2.3. **PCK2 silencing by siRNA**

Cells were transfected with 20 nM of non-silencing (ctrl) siRNA (Non-targeting pool, Dharmacon, Horizon, Colorado, USA), PCK2 siRNA1 (Smart pool PCK2, Dharmacon), a pool of 4 different siRNAs or PCK2 siRNA2, consisting of the following two sequences GGAUGAGGUUUGACAGUGA and UGGCUACAAUCCAGAGUAA (Dharmacon).

2.4. **PCK2 overexpression**

In PCK2 siRNA silenced cells, PCK2 was re-expressed by transfecting cells with 1 µg DNA per 200,000 cells of a PCK2 wild-type plasmid (Origene). The empty pCMV6-AC expression vector was used for control. Transfection occured 48 hours before the treatment.

2.5. **Stable isotopic tracing**

$^{13}C_5$-glutamine was used to trace TCA cycle metabolite interconversion and abundance. For treatment 2 mM $^{13}C_5$-glutamine (Sigma Aldrich) was added to glutamine free non-starvation or starvation treatment media. Cells were treated for 24 hours. Then, cells were rinsed with saline and instantly frozen on liquid nitrogen.

2.6. **Sample extraction**

A protocol for metabolite extraction and measurement was previously published (75). Metabolite extraction occurred on a mix of dry ice and ice. Ice-cold 62.5% methanol (Sigma Aldrich) in water, supplemented with norvaline (Sigma Aldrich) as an internal standard served as an extraction buffer. Cells were scraped and the lysate was transferred to a microcentrifuge tube, then ice-cold chloroform was added. Samples were either vortexed for 10 minutes at 4°C or sonicated 3 x 5 sec on ice. To separate the phases, centrifugation of the samples occurred at 13,000 rpm for 10 minutes at 4°C. To measure polar metabolites, the upper phase, meaning the methanol phase, was evaporated by vacuum centrifugation.

2.7. **Gas chromatography-mass spectrometry (GC-MS)**

To measure samples with GC-MS, samples were derivatized with 20 mg/mL methoxyamine in pyridine (both Sigma Aldrich) for 90 or 60 minutes at 37°C followed by N-(tert-butyldimethylsilyl)-N-methyl-trifluoroacetamide with 1% tert-Butyldimethylsilyl ethers (MTBSTFA + 1% TBDMS, Thermo Scientific) for 60 or 30 minutes at 60°C. Metabolite separation was performed with an Agilent 7890A GC system or an Agilent 7890B GC system. A DB35MS column and helium as carrier gas were used, the flow rate was 1 mL/minute. 1 µL of the sample was injected in splitless mode, the inlet temperature was set at 270°C. Temperature gradients for the respective devices are shown in Table 1. The GC system was connected to an Agilent 5975C or 5977A Inert MS system. An ionization energy of 70 eV was generated and m/z ranging from 100 to 650 atomic mass units were measured. Isotopologues were exported and correction for natural abundance was either performed by using a MATLAB Script (MA, USA) or IsoCor (76). Abundances were normalized to the respective protein content.

Table 1: GC-MS temperature gradients

Agilent 7890A GC system connected to Agilent 5975C Inert MS system	
Temperature	Temperature gradient
100 °C	hold for 1 minute
to 105 °C	2.5 °C/minute
to 240 °C	3.5 °C/minute
to 320 °C	2.5 °C/minute
320 °C	hold for 4 minutes

Agilent 7890B GC system connected to Agilent 5977A Inert MS system	
Temperature	Temperature gradient
100 °C	hold for 3 minutes
to 300 °C	3.5 °C/minute

2.8. **Liquid chromatography–mass spectrometry (LC-MS)**

The total abundance of GSH, GSSG, NADPH and $NADP^+$ was measured with LC-MS/MS. After vacuum centrifugation, samples were resuspended in 80% methanol (Sigma Aldrich) in water. Metabolites were separated by a Dionex UltiMate 3000 LC System (Thermo Scientific) with a HILIC column (iHILIC®-Fusion HILIC Column, SS, 150x2.1 mm, 1.8 µm, 100 Å). The

instrument was operated at 28°C. The applied gradient is shown in Table 2, left panel, whereas solvent A represented acetonitrile and solvent B was10 mM ammonium acetate, pH 9.3. The flow rate was set to 0.2 mL/minute. For detection, a negative scan mode using a spray voltage of 2.5 kV and a capillary temperature of 350°C, sheath gas was set at 50 and auxiliary gas at 10. To ensure specificity, for each metabolite two transitions were measured. Analysis was performed with the following transitions (precursor ion > product ion; collision energy): GSH (306>143; 20V), GSSG (611>306; 24V), NADPH (744>408; 40V), $NADP^+$ (742>273; 40V). Data collection and analysis was performed with Xcalibur software (Thermo Scientific).

Table 2: LC-MS solvent gradients

Dionex UltiMate 3000 LC System operated with a HILIC column		
Time (minutes)	% A	% B
0	92	8
2	92	8
7	65	35
16	58	42
26	25	75
28	25	75
30	92	8
38	92	8

Dionex UltiMate 3000 LC System operated with a C18 column		
Time (minutes)	% A	% B
0	100	0
2	100	0
7	63	37
14	59	41
26	0	100
30	0	100
31	100	0
40	100	0

Isotopologues of GSH were detected with LC–MS as published in (77). After vacuum centrifugation polar metabolites were resuspended in H_2O. Separation occurred with a Dionex UltiMate 3000 LC System (Thermo Scientific) utilizing a C18 column (Acquity UPLC HSS T3 1.8 µm 2.1 × 100 mm) at 40 °C, connected to a Q-Exactive Orbitrap (Thermo Scientific). A flow rate of 0.25 mL/minute was applied. The gradient is shown in Table 2, right panel, whereas solvent A is H_2O containing 10 mM tributyl-amine and 15 mM acetic acid and solvent represented methanol. For detection, a negative scan mode using a spray voltage of 4.9 kV was used and m/z ranging from 70 to 900 atomic mass units were measured. Collection and analysis were performed with the Xcalibur software (Thermo Scientific).

2.9. **Seahorse measurements**

40,000 cells per well were seeded on XF96 cell culture plates (Seahorse Bioscience, Agilent; CA, USA), previously coated with Cell-Tak™ (Corning, NY, USA). After 24 hours, cells were treated for 24 hours with starvation or non-starvation media. Media was either supplemented with 1 mM pyruvate (Sigma Aldrich) (experiment: H23 ctrl sh_v/PCK2sh_v and PCK2sh_mt cells) or 10 mM lactate (Sigma Aldrich) (all other measurements), serving as respiratory substrates, if not otherwise stated. A XF96 Extracellular Flux analyzer (Seahorse Bioscience) was utilized to record the oxygen consumption rate (OCR). Respiration was measured under basal conditions, after adding 2 µM oligomycin, 0.2 µM (H23)/0.5 µM (A549) carbonyl cyanide-4-(trifluoromethoxy) phenylhydrazone (FCCP) and 10 µM antimycin. Media was supplemented with 40 µM etomoxir (Sigma Aldrich) if stated. Recorded OCR values were normalized to the respective protein content.

2.10. **Confocal microscopy of mitochondria**

20,000 cells per well were seeded on glass bottom 8-well chamber slides (Ibidi, Gräfelfing, Germany). After 24 hours of treatment, cells were rinsed with PBS and incubated for 30 minutes with 100 nM Mitotracker Green in RPMI SILAC supplemented with arginine and lysine. Then, after washing, the respective treatment media was added back. Images were taken with a Nikon A1 confocal microscope (Vienna, Austria) and evaluated by ImageJ (National Institutes of Health (NIH)) by using the MiNa plugin (78).

2.11. **Mitotracker analysis by flow cytometry**

After 24 hours of treatment, cells were rinsed with PBS and cultured for 30 minutes with serum-free media containing 100 nM Mitotracker Green (Thermo Scientific). Afterwards, cells were rinsed with PBS and mitochondrial mass was analyzed in starvation media by flow cytometry (CytoFlex, BeckmanCoulter, Krefeld, Germany) in the FITC channel. Live and single cells were gated

2.12. **Detection of ROS**

Cells were treated for 24 hours with non-starvation or starvation media. To determine mitochondrial superoxide, cells were rinsed with PBS, trypsinized (Gibco) and incubated for 20 minutes with 2.5 µM of MitoSox (Thermo Scientific). Cells were then rinsed with PBS,

resuspended, and analyzed by flow cytometry. To detect general ROS, cells were incubated for 30 minutes with 10 µM CM-H2DCFDA (Thermo Scientific) followed by flow cytometry. Lipid peroxidation was analyzed in starved cancer cells with HBSS containing 2 µM Bodipy-C11 dye, followed by flow cytometry. If indicated RSL3 (Selleck chemicals, Houston, TX, USA) was added during treatment. Live and single cells were gated

2.13. **Detection of GSH/GSSG**

After 24 hours of treatment, cells were rinsed with PBS and homogenized in mammalian cell lysis buffer (Abcam, Cambridge, UK). Samples were deproteinized before measurement by using a TCA deproteinization kit (Abcam). The GSH/GSSG ratio of the samples was analyzed by a commercially available kit (Abcam), according to the manufacturer's descriptions.

2.14. **Colony formation assay**

Indicated numbers of cells were plated onto 6-well plates. After 24 hours, cells were rinsed two times and starvation or non-starvation media was applied for 72 hours. During the treatment, if stated, treatment media was supplemented with antioxidants or pro-oxidants at the concentrations indicated. Afterwards, cells could recover in normal growth medium (2 weeks for H23 cells, 10 days for A549 cells). Thereafter, colonies were fixed with methanol:acetic acid (3:1 v/v). Staining was performed with a 0.4 % crystal violet solution. Then the colony area was assessed with the ImageJ software (NIH) by using the Colony Area plugin (79).

2.15. **Cell counting**

75,000 (A549) or 100,000 (H23) cells/well were plated on 12-well plates. Then cells were treated for 24 hours with starvation medium containing indicated concentrations of H_2O_2 (Roth, Karlsruhe, Germany). For experiments with buthionine sulfoximine (BSO), BSO (Sigma Aldrich) was added to the the treatment media for 72 hours consistent with the treatment period of the colony formation assay. After the treatment, cells were washed with PBS, trypsinized and counting was performed with the Casy-TT cell counter (Roche Innovatis, Bielefeld, Germany).

2.16. **Proliferation**

After 24 hours of treatment with media containing 10 mM lactic acid, proliferating cells were detected by using the EdU Click-iT kit (Thermo Scientific). 10 µM EdU was added to the cells

and incubated for 1.5 hours. After collection, fixation and permeabilization cells were dissolved in the Click iT reaction cocktail as described in the manufacturer's protocol. Then cells were measured by flow cytometry; live and single cells were gated, and EdU-positive cells were determined.

2.17. **Western blot**

Cells were rinsed with PBS, lysis occurred with RIPA buffer (Thermo Scientific) containing protease inhibitor (Thermo Scientific) at 4°C. The cell extract was homogenized by sonication and centrifuged (maximum speed, 10 minutes, 4 °C). The concentration of the lysate was assessed with a BCA kit (Merck, Vienna, Austria). Protein was supplemented with Laemmli Buffer, incubated for 10 minutes at 95 °C. Then proteins were separated by sodium dodecyl sulfate-polyacrylamide gel electrophoresis by utilizing a Mini-PROTEAN® electrophoresis device (BioRad, Hercules, CA, USA). Subsequently, proteins were transferred to a polyvinylidene fluorid (PVDF) membrane (BioRad) or a nitrocellulose membrane (Thermo Scientific). Then the membrane was blocked for 1 hour either with 5 % BSA or milk (both Sigma Aldrich) dissolved in tris-buffered saline with 0.1% Tween 20 (TBST) as indicated in Table 3. Antibodies, described in Table 3, were diluted in the indicated blocking solution, and used for overnight incubation at 4°C. Anti-mouse and anti-rabbit secondary antibodies were used according to the primary antibody used. β-actin served as a loading control.

Table 3: Antibodies specifications

Antibody	Distributor	Blocking	Concentration
PCK2	Abcam, ab187145	BSA	1:2000
OXPHOS antibody cocktail	Abcam, ab 110411	milk	1:1000
TOM20	Cell Signaling Technology, #42406	milk	1:1000
SLC7A11	Abcam, ab175186	milk	1:1500
β-actin	Santa Cruz, sc-47778; Sigma, A5441	milk	1:3000

2.18. **Quantitative real-time PCR (RT-qPCR)**

RNA was extracted with the peqGOLD Total RNA kit (VWR, Vienna, Austria), according to the manufacturer's protocol and the RNA content was measured by spectrophotometry (NanoDrop, Thermo Scientific). Reverse transcription of total RNA was performed by using the qScript™ cDNA Synthesis kit (Quanta, Beverly, USA) as recommended by the manufacturer. For RT-qPCR the Blue S'Green qPCR Kit (Biozym, Vienna, Austria) was utilized on a LightCycler 480 (Roche, Vienna, Austria). Utilized primers are stated in Table 4.

Table 4: Primer sequences

Gene	Forward primer (5'-3')	Reverse primer (5'-3')
PCK2	CATCCGAAAGCTCCCCAAGTA	TGGAAATCAGCTGGGGACATC
GLS1	GAGTTGCTGGGGGCATTCT	TACACAGAGAAACAAGATCGTGACA
GLS2	GGCAGAGAGACGCCACA	CCTTTAGTGCAGTGGTGAACTT
GLUD1	CTCCAGACATGAGCACAGGTGA	CCAGTAGCAGAGATGCGTCCAT
ACLY	TGCTCGATTATGCACTGGAAGT	ATGAACCCCATACTCCTTCCCAG
NFE2L2	TGCCAACTACTCCCAGGTTG	AAGTGACTGAAACGTAGCCGA
GSR	CAGCGTCATTGTTGGTGCAG	CCTTGACCTGGGAGAACTTCAG
SLC7A11	TGACTGGAGTCCCTGCGTAT	TGTTCTGGTTATTTTCTCCGACATT
TXNRD1	CGATCTGCCCGTTGTGTTTG	TATTGGGCTGCCTCCTTAGC
UCP2	ACAAGACCATTGCACGAGAG	ATGAGGTTGGCTTTCAGGAG
SOD2	CCTCACATCAACGCGCAGATCA	ACAACCTGAACGTCACCGAGGA
GPX1	CCAAGCTCATCACCTGGTCT	TCGATGTCAATGGTCTGGAA
GPX4	TACCGGGGCTTCGTGTGCAT	TAGCCCGCGGCGAACTCTTT
SRXN1	CCTCGTGGACACGATCCG	CAGCCCCCAAAGGAGTAGAA
GLRX	AACAGAGTGGGGAACTGCTG	TGAACATTTCCTATGAGATCTGTGG
GSTP	GAGGGCTCACTCAAAGCCTC	GTCCTTCCCATAGAGCCCAAG
ACTB	ATTGCCGACAGGATGCAGGAA	GCTGATCCACATCTGCTGGAA

All primers were ordered from Eurofins Genomics (Vienna, Austria). ACTB expression was not different across all samples and thus served as reference gene. Amplification of the qPCR products was verified by analysis of the melting curves. Cp values were obtained by using the

2nd derivative method. The relative expression (ΔCp) was achieved by subtracting Cp values of the genes of interest from the Cp values of the reference gene (ACTB)

2.19. **Statistics**

Data compilation was performed with Microsoft Excel 2016, analysis was done with Microsoft Excel 2016 and SPSS, version 23.0 (Chicago, IL, USA). Groups were compared as applicable with two-sided, unpaired or paired Student's t-tests, one-group Student's t-tests or one-way ANOVA with Dunnett post-hoc analysis. p-values, smaller than 0.05 were considered as significant.

3. Results

3.1. PCK2 removes glutamine-derived TCA cycle intermediates

First, we compared the abundance of TCA cycle metabolites and their interconversion in NSCLC cells between nutrient replete and starvation conditions. The non-starvation media contained 10 mM glucose and 10% dialyzed FCS (dFCS) to provide full nutrient availability to the cells. For starvation treatment, a low concentration of glucose (0.2 mM) was used and serum was omitted, since it provides lipids and proteins, potentially metabolized by the cells. To trace the interconversion of TCA cycle intermediates we applied fully ^{13}C-labeled glutamine, as glutamine is described to be the major fuel of the TCA cycle (13,31). We treated H23 and A549 cells with the two different nutritional media and found that the amount of the TCA cycle metabolites fumarate or malate and citrate was decreased upon starvation treatment (Figures 5A and 6A). Under both conditions, glutamine fueled the TCA cycle and resulted in completely ^{13}C labeled malate and fumarate (M+4) however the fraction of labeled metabolites was enhanced by treatment with starvation media in H23 but not in A549 cells (Figures 5B, 5C, 6C and D). Citrate M+4 (denoting citrate with four ^{13}C atoms) results from the condensation of fully labeled OAA with unlabeled acetyl-CoA. Completely labeled Citrate (M+6) is generated from OAA (M+4) and labeled acetyl-CoA (M+2). Upon starvation treatment between 20 and 30 % of total citrate was fully labeled whereas under non-starvation conditions only a very small proportion was detectable (Figures 5B, 5C, 6C and 6D). Consistently, we also found glutamine derived and therefore M+3 labeled pyruvate upon starvation conditions, but not with non-starvation medium (Figures 5B, 5C, 6C, 6D). Therefore, by treating cells with starvation media, a higher rate of pyruvate was formed from TCA cycle metabolites and was subsequently metabolized to acetyl-CoA which has been also previously shown to occur upon glucose depletion (80). Pyruvate was either formed by malic enzyme (ME) from malate or via PEP formation by PEPCK and subsequent pyruvate generation by PK. Labeling patterns of the TCA cycle metabolites that can be observed after addition of $^{13}C_5$-glutamine, are illustrated in the scheme in Figure 5E. Together, these results show that glutamine is shuttled towards the TCA cycle in these cell lines in both, starvation and non-starvation conditions. Thus, $^{13}C_5$-glutamine is suitable to assess TCA cycle activity and the fueling of TCA cycle intermediates into the downstream gluconeogenesis pathway.

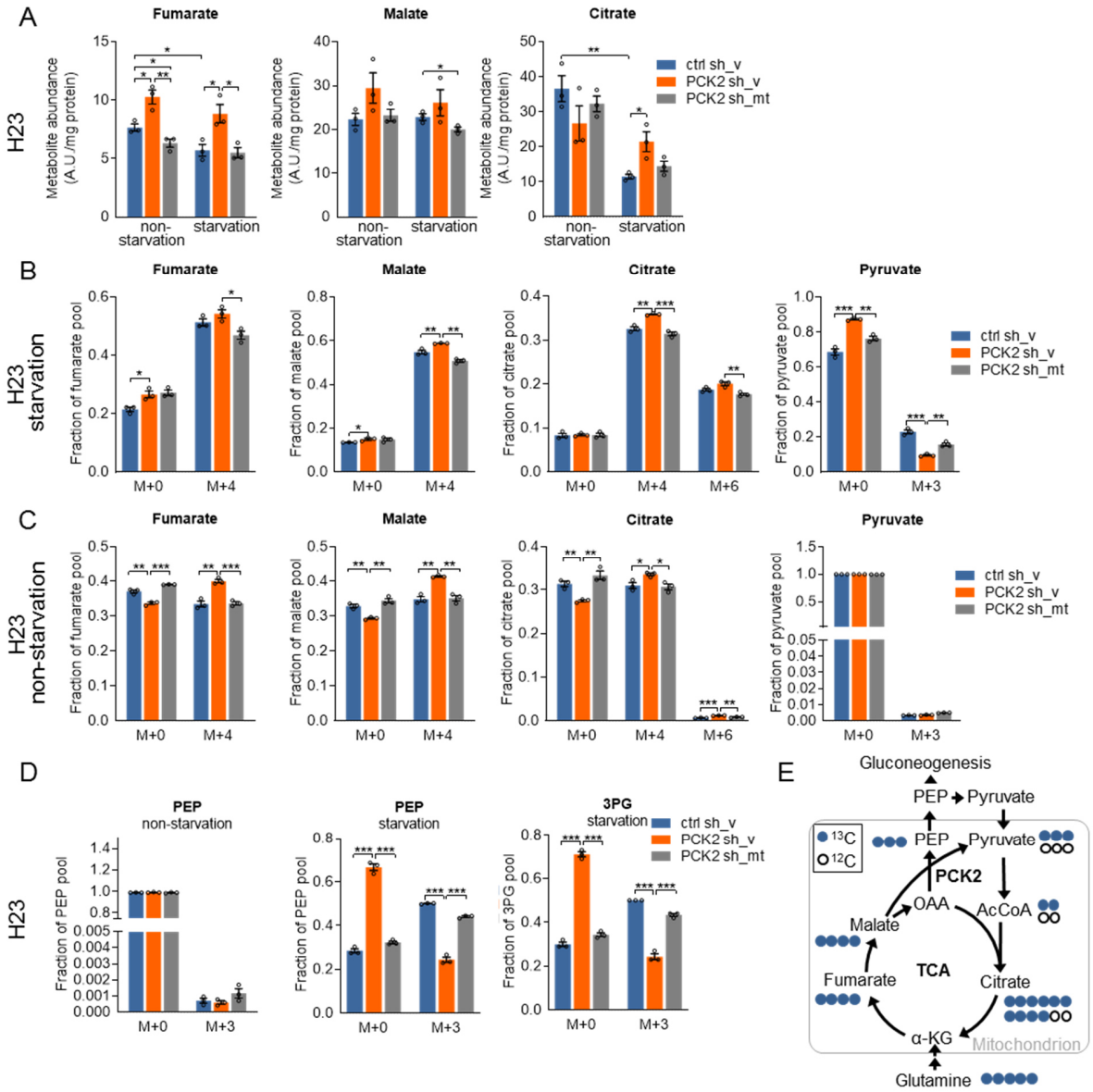

Figure 5: PCK2 expression influences the abundance and stable isotopic enrichment of TCA cycle metabolites and labeling of gluconeogenesis products in H23 cells. A) Control (ctrl sh_v), PCK2 silenced (PCK2 sh_v) or PCK2 re-expressing (PCK2sh_mt) H23 cells were cultured in non-starvation or starvation medium. Abundances of TCA cycle metabolites were measured. **B,C,D)** Stable isotopic enrichment with $^{13}C_5$-glutamine containing starvation (B,D) or non-starvation medium (C,D). **E)** Scheme for the interconversion of $^{13}C_5$-glutamine into the TCA cycle and the gluconeogenesis pathway. Data are displayed as mean ± SEM from three individual experiments. Comparison between groups was performed with two-sided, unpaired Student's t-tests. * p< 0.05, ** p<0.01, *** p<0.001. PEP, phosphoenolpyruvate; 3PG, 3-phosphoglycerate; A.U., arbitrary units. Figure panels reproduced from Bluemel et al., Free Radical Biology and Medicine, 2021 (1).

Next, we wanted to assess the role of PCK2 in regulating the TCA cycle upon starvation treatment. In H23 cells, PCK2 was silenced by stable expression of PCK2 shRNA (PCK2 sh). The silencing of PCK2 was rescued by the expression of a point mutated, PCK2 shRNA resistant allele (PCK2 sh_mt) (Figure 7B). In A549 cells, PCK2 expression was silenced with two different siRNA pools (Figure 7A) and PCK2 was re-expressed by concurrent overexpression of wild-type PCK2 in PCK2 silenced cells (Figure 7C). By addressing the amount of TCA cycle metabolites, we discovered, that PCK2 silencing elevated the abundance of fumarate, malate and citrate upon treatment with starvation media (Figures 5A and 6A). In both cell lines, the re-expression of PCK2 diminished the elevation by PCK2 silencing (Figures 5A and 6B). PCK2 silencing increased the amount of M+4 labeled citrate, malate and partly also of fumarate under non-starvation and starvation treatment in H23 cells, (Figure 5B and C). Similarly, in starved A549 cells, the level of M+4 labeling of malate and fumarate and of the M+6 isotopologue of citrate was elevated by PCK2 silencing while the effects were observed to a much smaller extent under non-starvation treatment (Figure 6C and 6D). In H23 cells, PCK2 silencing reduced the fraction of pyruvate M+3 labeling (Figure 5B), whereas in A549 cells pyruvate M+3 was increased (Figure 6C). These data show that in H23 cells PCK2 participates in OAA decarboxylation, whereas A549 cells seem to use an alternative route to convert TCA cycle intermediates to pyruvate, potentially via ME.

Glutamine fueling into the TCA cycle via the synthesis of glutamate from glutamine and the subsequent formation of α-ketoglutarate (α-KG), were not affected by PCK2 silencing (Figure 8A and B). Thus, altered glutaminolysis does not explain the enhanced TCA labelling upon PCK2 silencing. Upon non-starvation treatment, PCK2 silencing in H23 cells increased the levels of completely labeled glutamate and α-KG (M+5), M+4 labeled fumarate, malate and citrate and additionally the total abundance of α-KG and fumarate, whereas in A549 cells no differences were observed (Figures 5A, 5C and 8A-D). In non-starved H23 cells PCK2 induced a slightly increased expression of the enzyme of glutamine to glutamate conversion (*GLS1*) and a small but also insignificant reduction in the expression of the enzyme ATP citrate lyase (*ACLY*), that cleaves citrate into oxaloacetate and acetyl-CoA (Figure 8E).

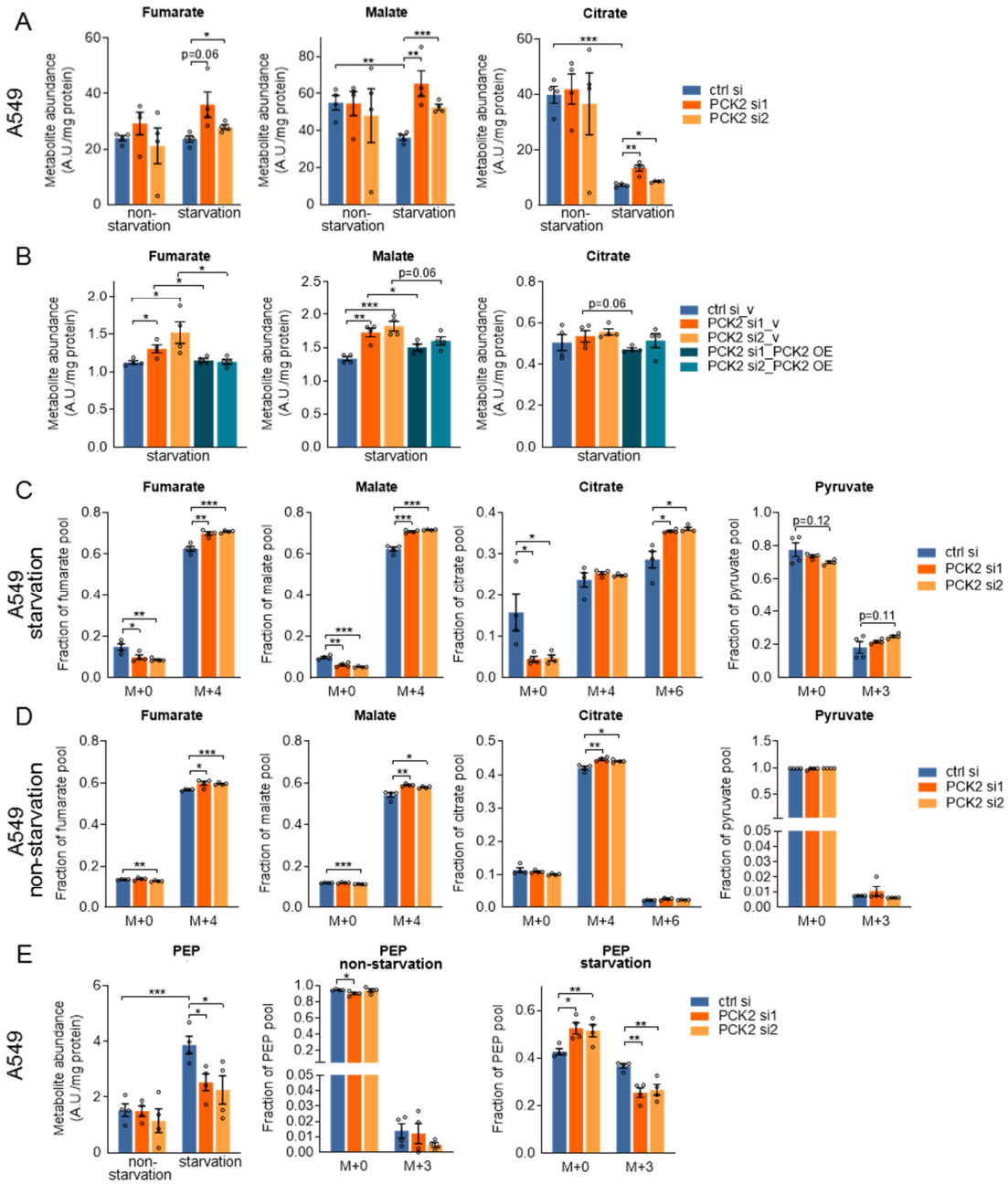

Figure 6: PCK2 expression has an impact on the abundance and the stable isotopic enrichment of TCA cycle intermediates and PEP in A549 cells A,E) A549 cells were transfected either with non-silencing ctrl siRNA (ctrl si) or with PCK2 targeting siRNA (PCK2 si1/PCK2 si2).Thereafter, cells were cultured in starvation medium or non-starvation medium and the abundance of TCA cycle metabolites and PEP was measured. **B)** TCA cycle intermediates abundance of starved cells, transfected as defined in (A) and in addition transfected with a control (v) or a PCK2 overexpressing (PCK2 OE) plasmid. **C,D,E)** Transfection occurred as described in (A) and stable isotopic enrichment after treatment with starvation (C,E) or non-starvation medium (D,E) supplemented with $^{13}C_5$-glutamine was measured. Data are displayed as mean ± SEM from four individual experiments. Groups were compared with two-sided, unpaired Student's t-tests. * p< 0.05, ** p<0.01, *** p<0.001. PEP, phosphoenolpyruvate; A.U., arbitrary units. Figure panels reproduced from Bluemel et al., Free Radical Biology and Medicine, 2021 (1).

Importantly, upon starvation treatment the PCK2 mediated gluconeogenesis pathway showed a high activity. After 24 hours of treatment, 40 - 50% of PEP and also of its downstream metabolite 3-phosphoglycerate (3-PG) was $^{13}C_5$-glutamine derived (Figures 5D and 6E). In contrast, upon treatment with non-starvation media, only 0.1-1% of PEP was labeled showing that gluconeogenesis was low under these conditions. In line with previous reports by our group, protein expression of PCK2 is increased under nutrient starvation treatment (Figure 7A), (41,44). In both cell lines PCK2 silencing diminished ^{13}C-labeling of PEP and 3PG (Figures 5D and 6E). In A549 cells, the abundance of PEP was increased when cells were cultured in starvation media and reduced by PCK2 silencing (Figure 6E). In summary, PCK2 silencing enhanced TCA cycle intermediate levels and interconversion, especially under starvation conditions. ^{13}C-labeling of the PCK2 downstream metabolites shows that this effect is attributable to a direct decrease of OAA by PCK2. Upon non-starvation treatment, however, a cell-line dependent PCK2-dependent modulation of anaplerotic and cataplerotic enzymes may be involved.

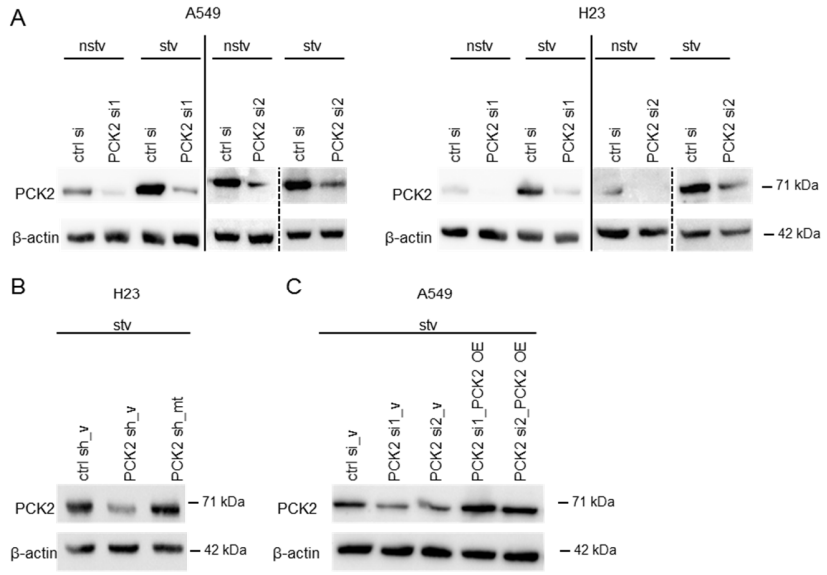

Figure 7: PCK2 expression is increased after treatment with starvation media. A) A549 and H23 cells were transfected with two different pools of PCK2 siRNA. Representative Western blots after 24 hours of treatment with non-starvation (nstv) or starvation (stv) media are shown. **B)** H23 cells that were stably expressing control shRNA (ctrl sh) or PCK2 shRNA (PCK2 sh) were transfected with the empty vector (H23 ctrl sh_v and PCK2 sh_v) or a shRNA resistant PCK2 allele (PCK2 sh_mt). A representative Western blot after treatment with starvation media, is shown. **C)** A549 cells, transfected as described in (A) were additionally transfected with a control (ctrl) or a PCK2 overexpressing (PCK2 OE) plasmid. A representative Western blot after treatment with starvation media is shown. (A-C) For all blots, β-actin was utilized as loading control. Figure panels reproduced from Bluemel et al., Free Radical Biology and Medicine, 2021 (1).

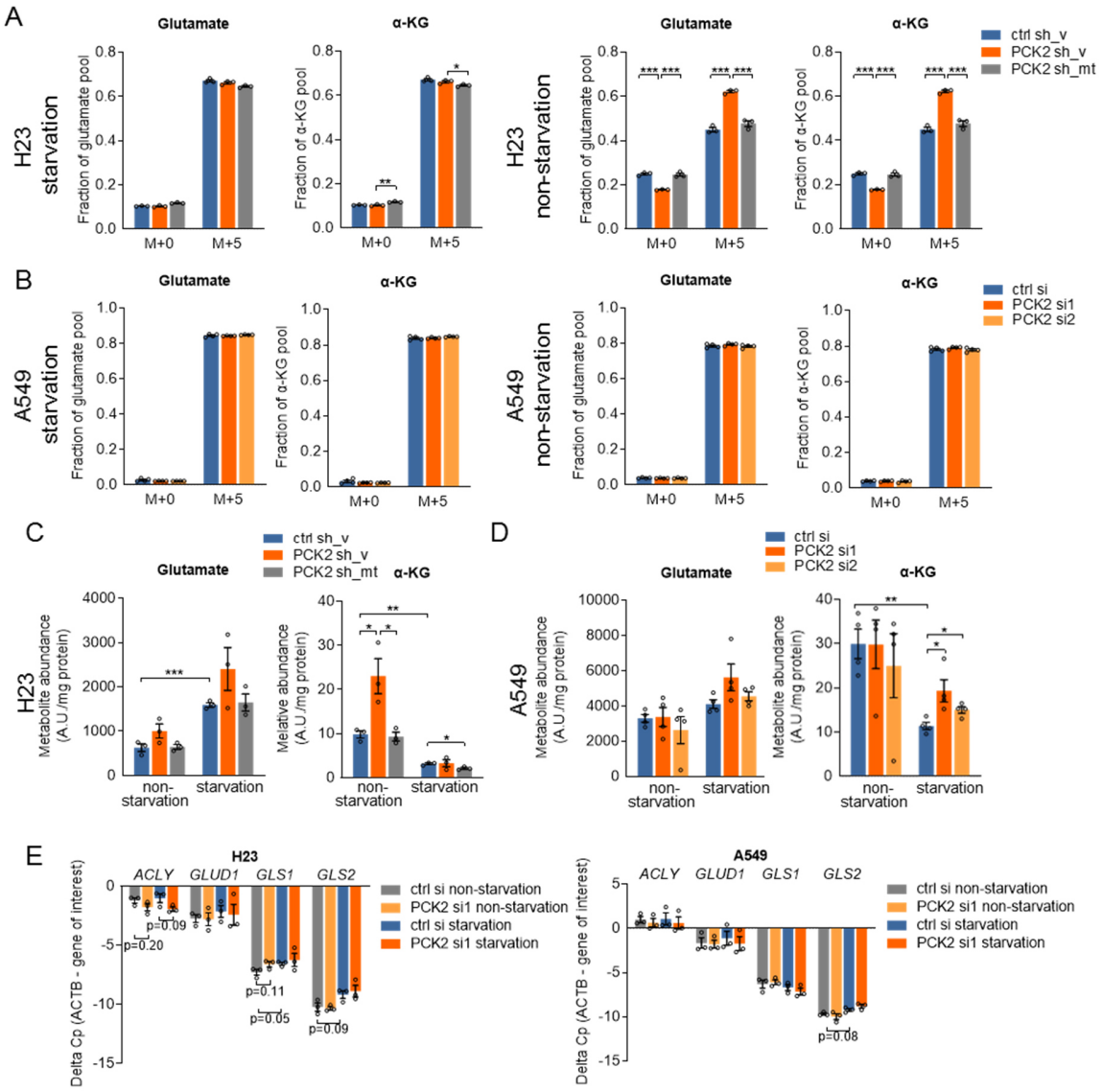

Figure 8: Influence of PCK2 expression on glutaminolysis and ana- or cataplerotic enzymes. A, B) Incorporation of $^{13}C_5$ glutamine into glutamate and α-ketoglutarate (α-KG) in H23 and A549 cells, transfected and treated as previously stated (A) n=3 and (B) n=4 individual experiments. **C,D)** Total abundance of glutamate and α-ketoglutarate (α-KG) in A549 and H23 cells. (C) n=3 and (D) n=4 experiments. A.U., arbitrary units. **E)** Expression of glutaminase (GLS1 and GLS2), glutamate dehydrogenase (GLUD1), and ATP citrate lyase (ACLY), was measured and normalized to ACTB. n=3 individual experiments. Results are mean ± SEM. Groups were compared by two-sided, unpaired Student's t-tests. * p< 0.05, ** p<0.01, *** p<0.001. Figure panels reproduced from Bluemel et al., Free Radical Biology and Medicine, 2021 (1).

3.2. PCK2 reduces mitochondrial respiration in starved cancer cells

The TCA cycle is not only a hub for biosynthetic intermediates but also yields the reducing equivalents NADH and $FADH_2$, which are then oxidized in the ETC during the process of mitochondrial respiration in order to generate ATP (81). When we compared oxygen consumption rates (OCR) in both cell lines between cells treated the two different nutritional media, we found an increased mitochondrial respiration in starved cells (Figure 9A). Upon starvation, PCK2 silencing further augmented basal and maximal OCR, but not ATP-linked respiration (Figures 9D-G). Therefore, additional oxygen consumed by PCK2 silenced cells seems to not be used for ATP generation (Figures 9D-G). Upon non-starvation treatment no significant effect of PCK2 silencing was discovered (Figures 9D-G). During OCR measurements, media was supplemented with pyruvate or lactate, serving as respiratory fuels. However, cells respired also without addition of pyruvate or lactate (starvation-lac, Figure 9B), and the increase of basal respiration through PCK2 silencing was comparable to cells treated with starvation media containing lactate. When etomoxir (Eto), which inhibits fatty acid oxidation, was added during the measurement, OCR decreased, showing that under nutrient deprivation, cells partly use fatty acids to fuel respiration (Figure 9C). Of note when fatty acid oxidation was blocked, PCK2 silencing increased oxygen consumption rates (Figure 9C). These data show that upon treatment with starvation media, PCK2 expression reduces mitochondrial respiration.

The mitochondrial morphology is affected by the nutritional status. Upon inappropriate nutrient supply, mitochondria have a tendency to be elongated as this induces OXPHOS and guards from autophagosomal degradation (82,83). When we assessed mitochondrial morphology, the number of individual mitochondria was not altered by treatment with the two different nutritional media, however, in starved cells PCK2 silencing led to a decreased number of individual mitochondria (Figure 10A). The mitochondrial mass remained unaffected by starvation treatment and by PCK2 silencing (Figure 10B). Together these results hint that PCK2 silencing might cause mitochondrial elongation. Interrogating if enhanced mitochondrial respiration by PCK2 silencing is mediated by upregulation of ETC complex members, we analyzed the protein levels of key electron transport chain subunits from the five different mitochondrial complexes (I to V). However, expression of NDUFB8, SDHB, UQCRC2, COX II and ATP5A as well as of the mitochondrial import protein TOM20 were not affected by PCK2 siRNA (Figures 10C and

D). Accordingly, enhanced respiration by PCK2 silencing is likely caused due to its impact on the TCA cycle activity than as a consequence of increased expression of OXPHOS proteins.

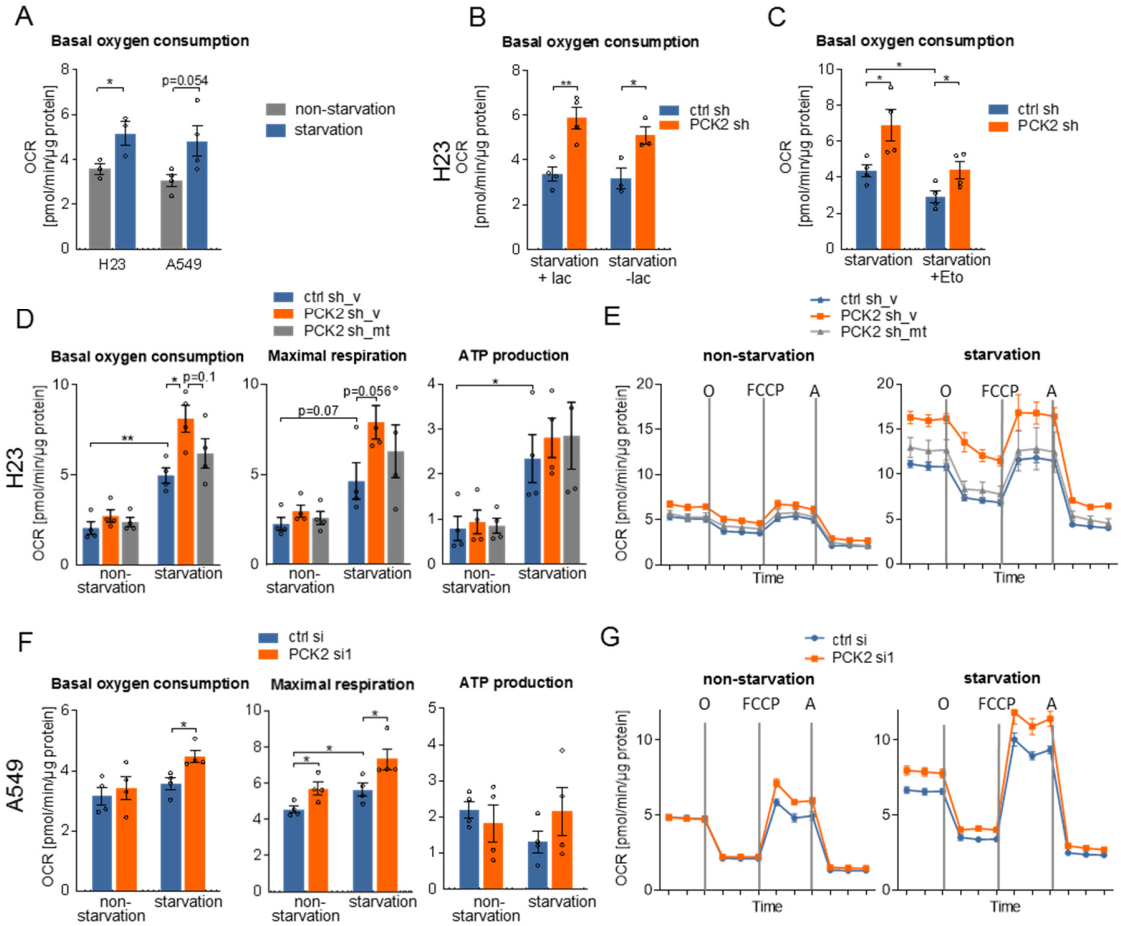

Figure 9: Mitochondrial respiration is enhanced by PCK2 silencing. A) Basal oxygen consumption rate (OCR) was measured in non-starved or starved H23 and A549 cells. **B,C)** OCR of control (ctrl sh) or PCK2 silenced (PCK2 sh) starved H23 cells, with or without lactate supplementation (B) or with or without etomoxir (Eto) addition (C). **D,F)** Basal OCR, maximal OCR and ATP-production-linked OCR was measured in non-starved or starved H23 or A549 cells, transfected as previously described. **E,G)** Representative OCR measurements showing respiration at the basal state and after the addition of oligomycin (O), FCCP and antimycin (A). Representative recordings that display the mean ± SEM of five or six technical replicates are shown. (A-D,F) The mean ± SEM from n=4 experiments, each combining four to six technical replicates, is shown. Group comparisons were performed by two-sided, unpaired Student's t-tests. * p< 0.05, ** p<0.01. Figure panels reproduced from Bluemel et al., Free Radical Biology and Medicine, 2021 (1).

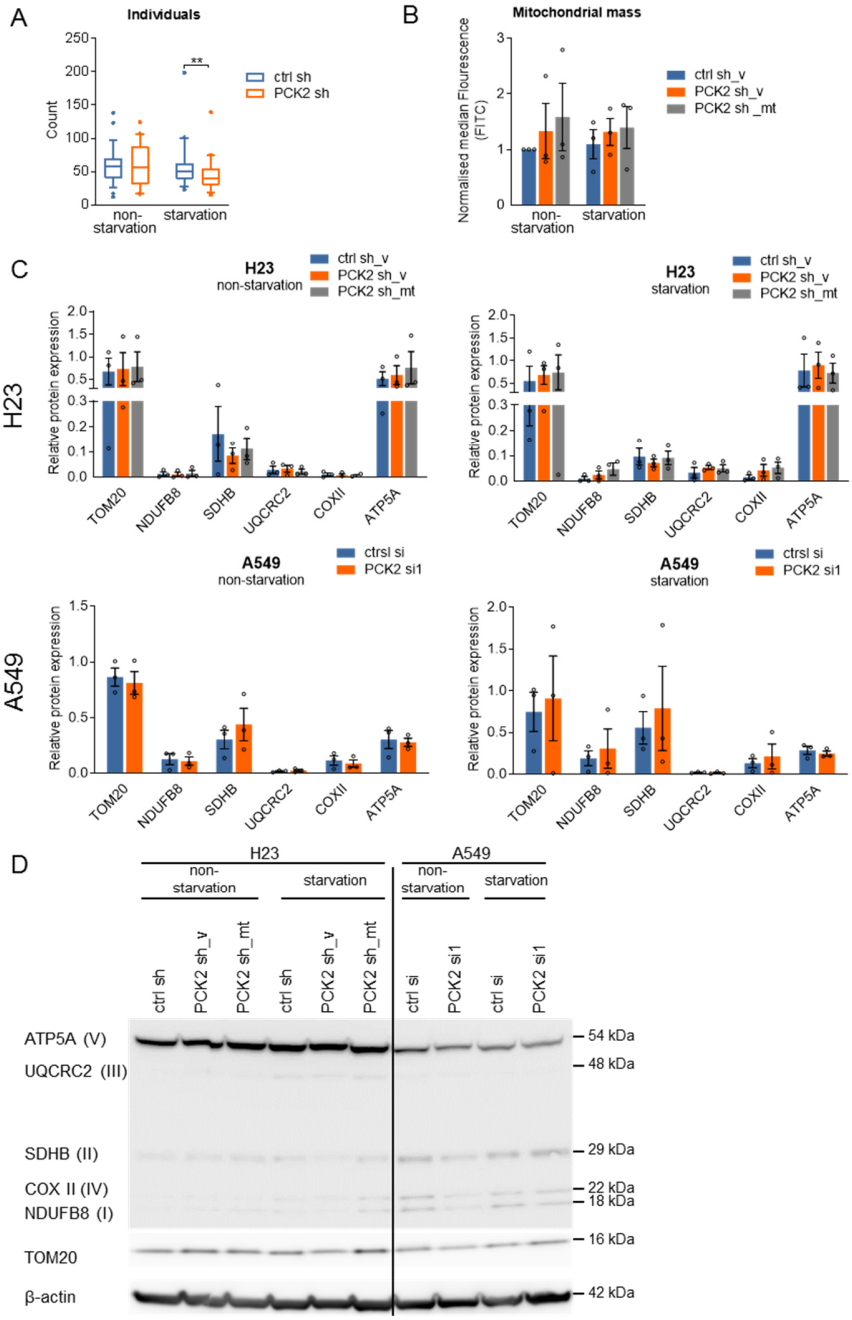

Figure 10: Influence of PCK2 expression on mitochondrial morphology and mass and expression of OXPHOS proteins. A) Mitochondrial individuals in control (ctrl sh) or PCK2 silenced (PCK2 sh) H23 cells, cultured in non-starvation or starvation media. 39-59 cells from three independent experiments were analyzed per group. **B)** Mitochondrial mass of control (ctrl sh_v), PCK2 silenced (PCK2 sh_v) or PCK2 re-expressed (PCK2sh_mt) starved or non-starved H23 cells. **C,D)** Expression of respiratory chain complex subunits of H23 cells, as described in (B) or control (ctrl si) or PCK2 silenced (PCK2 si1) A549 cells. Levels were normalized to β-actin and a representative Western blot is shown. Data are shown as mean ± SEM from n=3 independent experiments. Comparisons between groups were done by two-sided, unpaired Student's t-tests or one-group Student's t-tests as applicable. ** p<0.01. Figure panels reproduced from Bluemel et al., Free Radical Biology and Medicine, 2021 (1).

3.3. PCK2 maintains the redox equilibrium under starvation

Mitochondrial respiration is the main origin of eventually damaging ROS that are constantly neutralized through antioxidant enzymes by oxidizing NADPH and GSH (12,63,84). We found that a 24 hour treatment period with starvation media in both cell lines led to the upregulation of the key regulator of the antioxidant defense *NFE2L2* (Figure 11A). Additionally, the expression of *GSR* and of the cysteine transporter subunit *SLC7A11* was increased upon starvation treatment (Figure 11A). PCK2 silencing with PCK2 si1 suppressed starvation induced SLC7A11 expression however silencing with PCK2 si2 or with PCK2 sh showed no difference (Figure 11A). At a protein level, SLC7A11 expression was not affected by PCK2 silencing (Figure 11B)

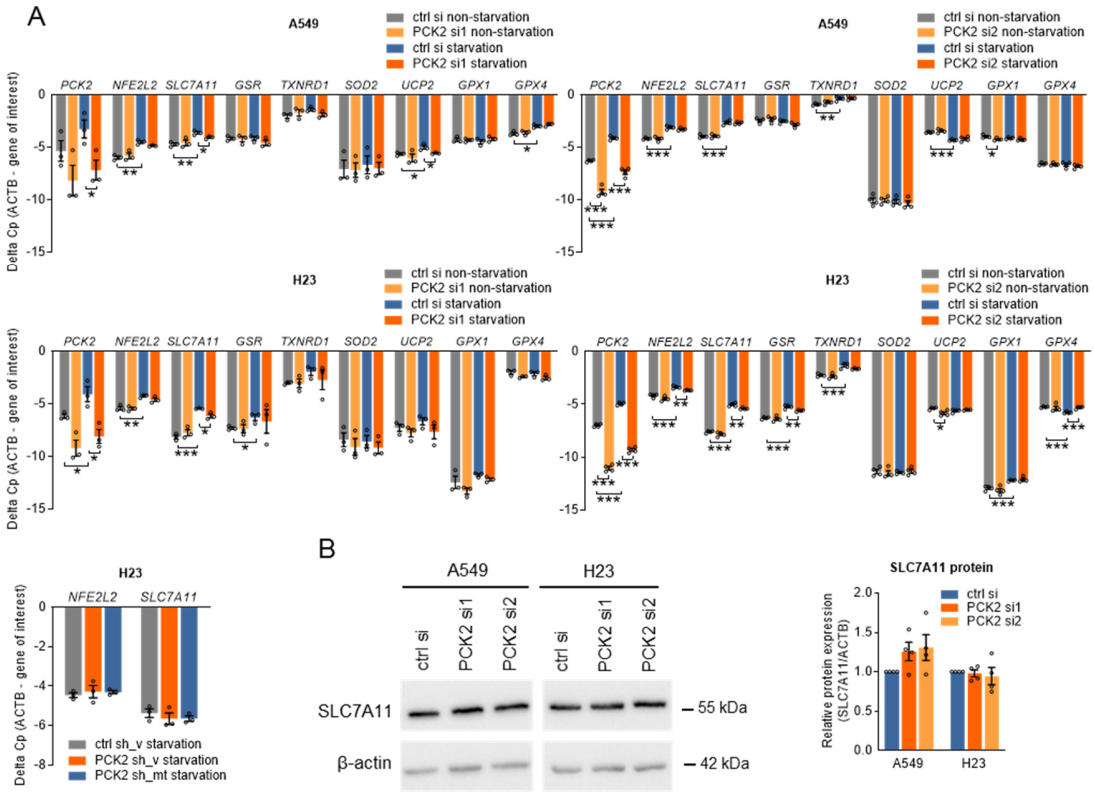

Figure 11: Expression of antioxidant genes is increased through treatment with starvation media and is in part influenced by PCK2 expression. A) mRNA expression of PCK2 and of different antioxidant defense genes (normalized to ACTB) in control (ctrl si) or PCK2 silenced (PCK2 si1, PCK2 si2) H23 and A549 cells and of control (ctrl sh_v), PCK2 silenced (PCK2 sh_v) or PCK2 re-expressed (PCK2sh_mt) H23 cells. Cells were cultured in non-starvation or starvation media as indicated. **B)** SLC7A11 expression in control or PCK2 silenced starved A549 or H23 cells, was analyzed by Western blot. β-actin was utilized as loading control. Data are mean ± SEM from n=3 (PCK2 si1, PCK2 sh) or n=4 (PCK2 si2 and (B)) experiments. Group comparisons were performed with two-sided, unpaired Student's t-tests or one group Student's t-test as applicable. * p< 0.05, ** p<0.01, *** p<0.001. Figure panels reproduced from Bluemel et al., Free Radical Biology and Medicine, 2021 (1).

Next, we investigated if enhanced mitochondrial respiration caused by starvation treatment, which was additionally augmented by PCK2 silencing, modulates ROS levels. We assessed mitochondrial ROS and detected in H23 but not in A549 cells an increase in mitochondrial superoxide upon starvation treatment, that was not significantly increased by PCK2 silencing (Figure 12A). Similarly, when we measured DCFDA oxidation, an indicator of cellular ROS, starvation treatment and PCK2 silencing caused a small, but insignificant increase in ROS levels (Figure 12B). However, the ratio of reduced to oxidized GSH (GSH/GSSG) was decreased by PCK2 silencing upon starvation media, as shown by two different methods (Figure 12C). Additionally, the NADPH/$NADP^+$ ratio was diminished by PCK2 silencing upon starvation treatment (Figure 12D). Lipid peroxidation was slightly reduced by PCK2 silencing in starved H23 cells. However, if GPX4, the enzyme reducing lipid peroxidation at the expense of GSH, was blocked through the addition of RSL3, PCK2 silencing increased lipid peroxidation levels (Figure 12E). This demonstrates high ROS levels, which are continuously balanced by GPX4 by oxidizing GSH. As the expression of antioxidant enzymes is increased upon treatment with starvation media and the GSH/GSSG ratio is decreased, we concluded that ROS, generated by the ETC upon PCK2 silencing were scavenged by antioxidant defense mechanisms which leads to a reduced glutathione redox capacity. In H23, but not in A549 cells, enhanced GSH oxidation caused by PCK2 silencing was also found upon treatment with non-starvation media (Figure 12C). These conditions also enhanced the levels and interconversion of TCA cycle metabolites (Figures 5A and C) whereas oxygen consumption was only insignificantly enhanced (Figure 9D). Possibly, enhanced TCA cycle intermediates might cause enhanced ROS levels, unrelated to a forward oxidation in the ETC, e.g. by succinate-fueled reverse-electron flow (85).

GSH levels are either restored by reducing GSSG to GSH or they are *de novo* formed from glycine, cysteine and glutamate (68). Upon starvation, in H23 cells but not in A549 cells PCK2 silencing caused a slightly diminished level of GSH *de novo* biosynthesis, as indicated by a higher abundance of GSH M+0 (Figure 12F). GSH M+5 found upon starvation treatment likely indicates labeled glutamate (5 carbon units), which is directly ^{13}C-glutamine derived. Under our experimental conditions, a incorporation of ^{13}C from glutamine into serine or glycine was not detected in H23 cells and only to a minor extent in A549 cells (data not shown). Therefore, higher GSH isotopologues were not examined.

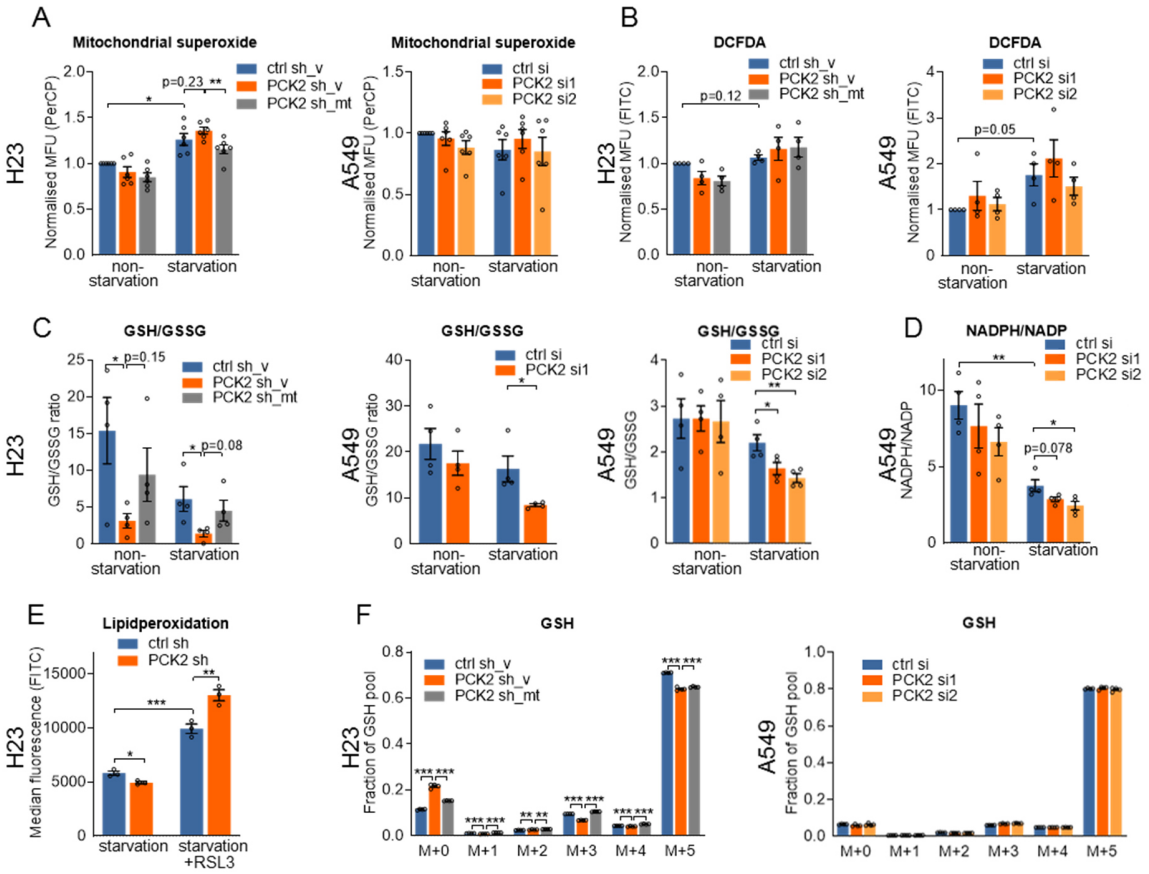

Figure 12: The ratio of reduced to oxidized glutathione is highly decreased by PCK2 silencing. A) Mitochondrial superoxide was measured in ctrl sh_v, PCK2 sh_v or PCK2 shRNA expressing H23 cells and in A549 cells transfected with ctrl si or PCK2 si1/2. Cells were cultured in non-starvation or starvation medium. **B)** CM-H_2DCFDA oxidation, analyzed in H23 and A549 cells, transfected and treated as described in (A). **C)** Ratio of reduced to oxidized glutathione (GSH/GSSG) in H23 and A549 cells cultured as described in (A). Data of the two panels on the left were analyzed with a kit, data of the right panel were measured by LC-MS/MS. **D)** NADPH/NADP ratio in A549 cells, treated as described in (A), and measured by LC-MS/MS. **E)** Lipid peroxidation, measured in starved control (ctrl sh) or PCK2 silenced (PCK2 sh) H23 cells with or without addition of RSL3, a glutathione peroxidase 4 inhibitor. **F)** Fractional enrichment of isotopologues of glutathione (GSH; M+1 to M+5) of H23 and A549 cells transfected as described in (A) and treated with starvation media including $^{13}C_5$ glutamine. Data are mean ± SEM from n=6 (A), n=4 (B;C;D,F) and n=3 (E) independent experiments. Comparison between groups was performed with two-sided, unpaired Student's t-tests or one group Student's t-test as applicable. * p< 0.05, ** p<0.01, *** p<0.001. Figure panels reproduced from Bluemel et al., Free Radical Biology and Medicine, 2021 (1).

3.4. PCK2 expression is beneficial for colony formation and enhances resistance towards hydrogen peroxide

We studied the effect of PCK2 on cellular survival and proliferation under dense and loose plating. Colony formation of loosely plated cells is an important assay assessing the ability of single cells to survive a period of metabolic stress and their capability to proliferate thereafter. For colony formation, cells were initially treated with starvation or non-starvation media, then cells were allowed to recover and form colonies in growth medium. PCK2 silencing reduced colony formation of sparsely plated cells upon treatment with starvation media in both cell lines and in H23 cells additionally also under non-starvation treatment (Figure 13A). Upon normal, confluent, plating densities, PCK2 silencing had no effect on proliferation and cell numbers (Figures 13B and C). Next, we investigated if PCK2 expression protects tumor cells from H_2O_2 induced damage. In starved H23 and A549 cells, PCK2 silencing enhanced the toxicity of lower amounts of exogenously added H_2O_2 (Figure 13C). To identify, if a redox imbalance leads to reduced colony formation of PCK2 silenced cells, we supplemented the starvation or non-starvation media with antioxidants during the treatment period. We exogenously added trolox, a derivative of vitamin E, GSH and N-acetyl cysteine (NAC), a direct antioxidant but also a precursor of GSH and all three rescued the reduced colony forming potential caused by PCK2 silencing (Figures 13D and E).

The effect of PCK2 silencing is highly different when comparing proliferation and cell numbers of confluent cells to sparsely plated, colony forming, cells, an assay that requires cell survival and proliferation. So, we hypothesized that cancer cells under colony forming conditions are more susceptible to oxidation. We supplemented the treatment media with buthionine sulfoximine (BSO), which inhibits the first step of glutathione synthesis and induces oxidative stress. Whereas the colony forming ability upon non-starvation and starvation conditions was highly reduced by different BSO concentrations, the same concentrations only mildly influenced cell numbers of confluent cells (Figures 14A and B).

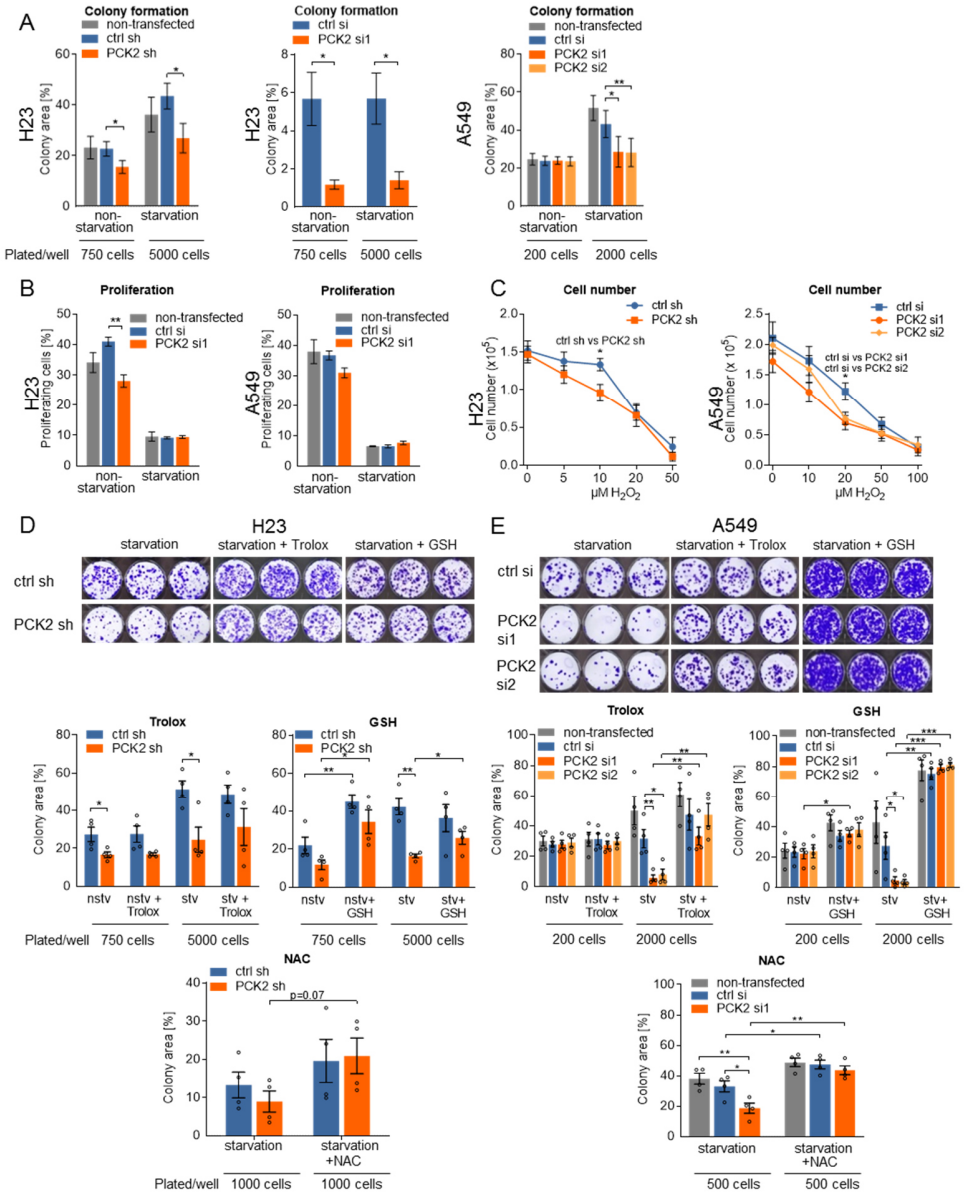

Figure 13: PCK2 silencing decreases the colony forming potential which can be rescued by antioxidants and renders more sensitive towards H_2O_2. A) Colony forming capability of loosely seeded control or PCK2 silenced H23 and A549 cells. Treatment occurred for 72 hours with non-starvation (nstv) or starvation (stv) media before recovery in full growth media. n=8 (H23 shRNA), n=4 (H23 siRNA), n=12 (A549) independent experiments, consisting out of three technical replicates. **B)** Proliferation of confluent control or PCK2 silenced starved or non-starved cells, n=3 independent experiments. **C)** Cell number of confluent, starved cells, supplemented with indicated concentrations of H_2O_2; n=4 experiments, performed in duplicates. **D,E)** Colony area of control or PCK2 silenced H23 or A549 cells, treated as described in A). If indicated, antioxidants were added during the treatment period at following concentrations: Trolox (100 μM), glutathione (GSH, 2 mM), and N-acetyl cysteine (NAC, 10 mM (D), 5 mM (E)). n=4 independent experiments, each done in technical triplicates. Data are shown as mean ± SEM. Comparison between groups was achieved by two-sided, unpaired or paired Student's t-tests as applicable. * p< 0.05, ** p<0.01, *** p<0.001. Figure panels reproduced from Bluemel et al., Free Radical Biology and Medicine, 2021 (1).

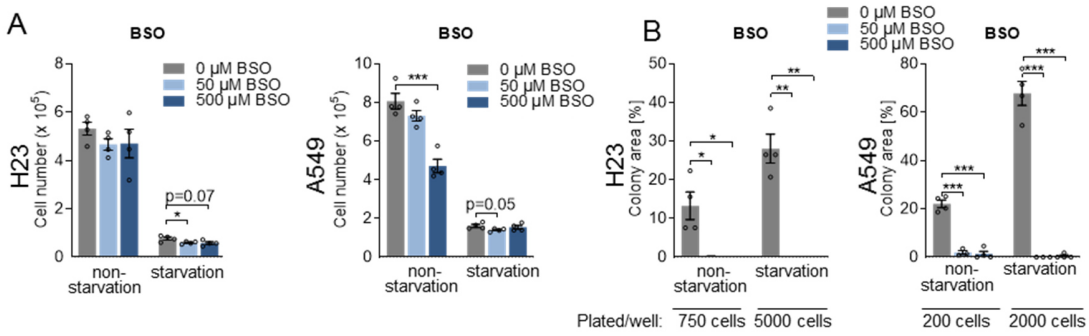

Figure 14: Colony formation is inhibited by addition of glutathione biosynthesis inhibitor buthionine sulfoximine (BSO). A) Cell number of densely plated H23 or A549 cells, cultured for 72 hours with non-starvation or starvation media supplemented different concentrations of BSO. **B)** Colony area of loosely plated A549 or H23 cells, cultured for 72 hours in non-starvation or starvation media supplemented with indicated concentrations of BSO. Data are displayed as mean ± SEM from n=4 individual experiments, consisting out of two (A) or three (B) technical replicates. Comparisons between groups were performed using two-sided Student's t-tests * p< 0.05, ** p<0.01, *** p<0.001. Figure panels reproduced from Bluemel et al., Free Radical Biology and Medicine, 2021 (1).

3.5. PCK2 silencing is mimicked by the addition of the TCA cycle precursor dimethyl malate

To investigate if enhanced TCA interconversion followed by augmented mitochondrial respiration caused a GSH/GSSG imbalance we fueled the TCA cycle with dimethyl-L-malate (DMM), a cell membrane permeable analogue of malate. In H23 cells, the addition of 5 mM of DMM caused increased respiration and reduced GSH/GSSG levels whereas superoxide levels were not significantly affected (Figures 15A-C). Additionally, DMM phenocopied the role of PCK2 silencing on the colony forming ability (Figure 15D). These effects were also discovered to a minor extent in A549 cells (Figures 15A-D). Potentially, the less pronounced impact of DMM addition in A549 cells can be connected to an enhanced removal of TCA metabolites via ME, which produces mitochondrial NADPH. These data reveal that the cataplerotic role of PCK2 contributes to the maintenance of the GSH/GSSG equilibrium by limiting TCA cycle activity and mitochondrial respiration.

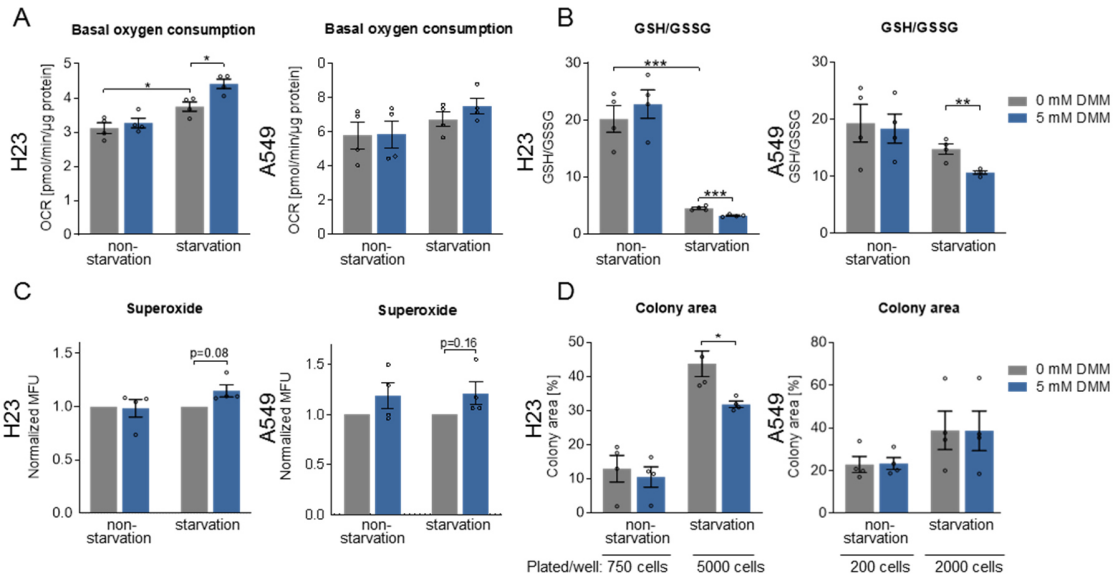

Figure 15: Addition of dimethyl-L-malate (DMM) phenocopies PCK2 silencing. Treatment media of H23 and A549 cells was supplemented with 5 mM dimethyl-L-malate (DMM). **A)** Basal oxygen consumption, **B)** GSH/GSSG ratio and **C)** mitochondrial superoxide were measured; Results are shown as mean ± SEM from n=4 individual experiments. **D)** Colony formation in loosely plated cells, treated with non-starvation or starvation media with or without DMM. Data are mean ± SEM from n=4 experiments, performed in triplicates. Groups were compared with two-sided, unpaired Student's t-tests or one group Student's t-test as applicable. * p< 0.05, ** p<0.01, *** p<0.001. Figure panels reproduced from Bluemel et al., Free Radical Biology and Medicine, 2021 (1).

3.6. PCK2 silencing is mimicked through the protein glutathionylation mediator diamide

An altered GSH/GSSG ratio can, independently of its direct effect on cellular damage by ROS, lead to GSSG-induced modifications and therefore contributes to the suppressive effect of PCK2 silencing on the colony forming ability through GSSG-induced modifications. Elevated GSSG levels were reported to induce S-glutathionylation of proteins (86). To investigate if protein S-glutathionylation causes diminished colony formation by PCK2 silencing, we supplemented the treatment media with diamide, an S-glutathionylating agent. In a dose-dependent manner, diamide decreased colony formation upon treatment with starvation media, while the colony forming potential was not affected in non-starvation media (Figure 16A). This suggests that nutrient deprived colony forming cancer cells are more vulnerable towards glutathionylation. Moreover, in both cell lines the protein de-glutathionylation enzymes

sulfiredoxin (*SRXN1*) and glutaredoxin-1 (*GLRX*) were upregulated upon treatment with starvation media whereas glutathione S-transferase P (*GSTP*), which selectively glutathionylates proteins, was expressed at the same level (Figure 16B).

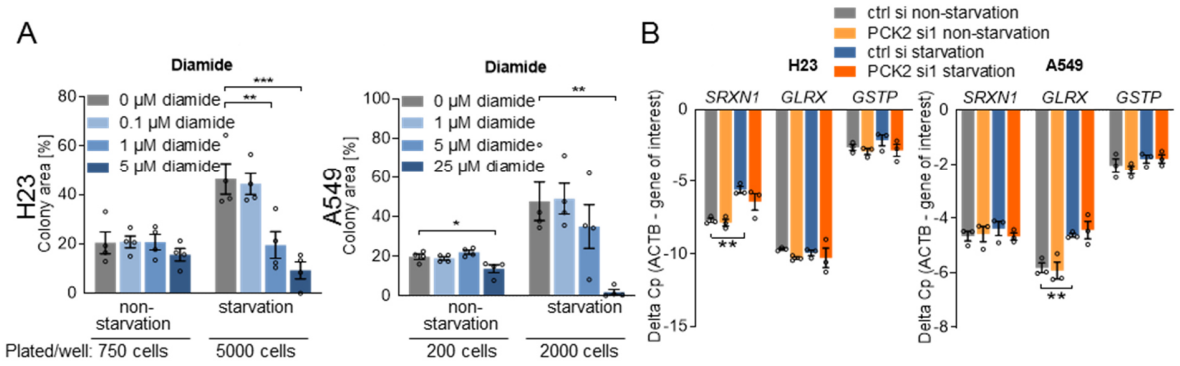

Figure 16: Colony formation is impaired by diamide, an inducer of glutathionylation. A) Colony area of loosely seeded H23 and A549 cells and treated with non-starvation or starvation media with or without diamide. Data are mean ± SEM from n=4 consisting out of three technical replicates **B)** mRNA expression of the glutathionylation modifying enzymes, sulfiredoxin (SRXN1), glutaredoxin-1 (GLRX) and glutathione S-transferase P (GSTP). Expression was normalized to β-actin (ACTB). Data are shown as mean ± SEM from n=3 experiments. Comparison between groups was performed using one-way ANOVA with Dunnett post hoc analysis or two-sided Student's t-tests. * p< 0.05, ** p<0.01, *** p<0.001. Figure panels reproduced from Bluemel et al., Free Radical Biology and Medicine, 2021 (1).

4. Discussion

Nutrient starvation forces cancer cells to acquire adaptations to survive (13,26). In recent years, the gluconeogenesis pathway via PCK2 was shown to be present in tumor cells, and its growth advantage in *in vitro* and in *in vivo* studies was revealed (41,43,44). Gluconeogenesis adds an important piece to the understanding of how cancer cells adapt to varying nutrient conditions and starvation. Here the role of PCK2 beyond the synthesis of gluconeogenic intermediates was identified in glucose and serum starved cancer cells, namely its importance as a cataplerotic enzyme. By mediating gluconeogenesis PCK2 removes TCA cycle intermediates which subsequently regulates mitochondrial respiration and the redox balance in nutrient deprived lung cancer cells. A model for PCK2's cataplerotic role and its subsequent regulatory function is shown in Figure 17.

4.1. Starvation media resembles a nutrient deprived microenvironment

For all experiments described here, cells were treated with non-starvation or starvation media. Non-starvation media contained 10 mM glucose and was additionally supplemented with 10% dFCS and should resemble conditions of high nutrient availability. To simulate severe nutrient shortage, starvation media consisted out of 0.2 mM glucose and serum was omitted. Glucose was not fully removed as this leads to rapid cell death, precluding experiments with a treatment period of 24 hours. Moreover, a severe reduction but not complete lack of glucose might more closely reflect the situation *in vivo*. The contributions of glucose or serum deprivation were not separately investigated in this study, as this would be highly laborious and make data interpretation difficult. In previous studies combined glucose and serum starvation showed the highest increase in PCK2 expression, compared to non-starvation conditions (41,44). Moreover, glucose deprivation is supposed to occur alongside a decrease in macronutrients and lipids in the tumor microenvironment, which is mimicked by serum starvation. Thus, we focused on nutrient poor (low glucose and serum free conditions) and conditions of full nutrition with a high glucose and serum availability. However, whether glucose, serum or combined starvation leads to differences between non-starvation and starvation treatment certain experiments remains to be clarified.

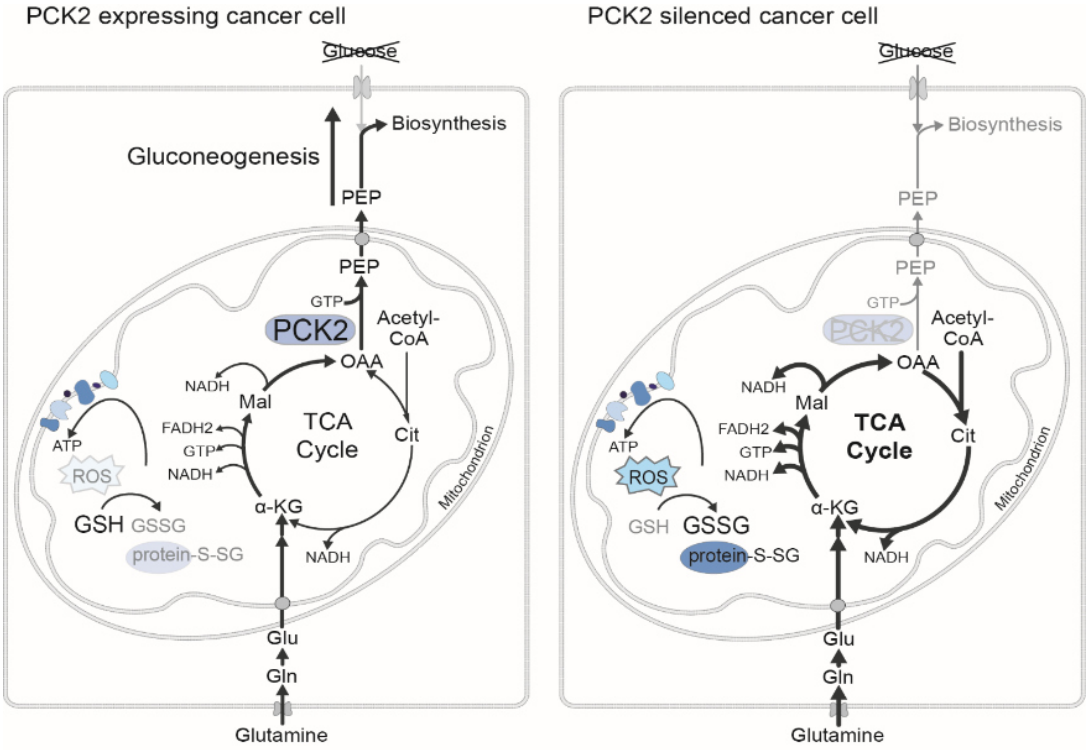

Figure 17: Model of the role of PCK2 on cataplerosis, mitochondrial respiration and the redox balance. Upon limited glucose availability, the gluconeogenic enzyme PCK2 synthesizes PEP (phosphoenolpyruvate) from OAA (oxaloacetate) and therefore removes tricarboxylic acid (TCA) cycle intermediates. Thereby, mitochondrial respiration is repressed which maintains the glutathione redox equilibrium. Figure panels reproduced from Bluemel et al., Free Radical Biology and Medicine, 2021 (1).

4.2. The cataplerotic role of PCK2 suppresses TCA cycle activity

We found that NSCLC cancer cells convert glutamine into TCA cycle intermediates in both nutitional media. After 24 hours of treatment, around 60% of TCA cycle intermediates were glutamine derived. PCK2 silencing caused increased cellular glutamine incorporation upon treatment with both media. Additionally, the amount of TCA cycle metabolites was enhanced by PCK2 silencing upon starvation treatment. The re-expression of PCK2 blunted the increased abundance of TCA cycle metabolites and glutamine incorporation.

Surprisingly, in both cell lines upon treatment with non-starvation media, PCK2 silencing enhanced ^{13}C labeling of TCA cycle metabolites and in H23 cells also to an increased abundance of fumarate and partly also of malate. Additionally, in H23 cells incorporation of

glutamine into glutamate and α-KG was increased by PCK2 silencing upon non-starvation treatment. PCK2 activity in direction of gluconeogenesis was very low upon non-starvation treatment as shown by $^{13}C_5$-glutamine tracing, still this activity might affect the TCA cycle. In line with these findings, a low level of PEPCK activity was detectable in lung cancer cells under high glucose conditions (41).

Recent studies, either showing a growth supportive or inhibiting role of PEPCK, identified the enzyme's influence on the TCA cycle, however the impact of PCK2 on glucose and serum starved cells was not investigated so far. Similar to our results in nutrient deprived lung cancer cells, in tumor initiating melanoma and prostate cancer cells and in hypoxic breast cancer cells upon growth in nutrient replete media, PCK2 silencing enhanced the amount of TCA cycle metabolites (45,49,61). However, in these studies $^{13}C_5$-glutamine conversion into TCA cycle intermediates was not investigated. In prostate cancer cells, reduced abundance of the TCA cycle intermediate citrate by PCK2 expression was connected to reduced protein acetylation and led to enhanced proliferation. However, in melanoma cells, PCK2 expression also reduced the citrate levels but caused growth inhibition. In the hypoxic breast cancer model, PCK2 overexpression reduced TCA cycle intermediates but also ROS formation and resulted in a growth arrest (61). Surprisingly, in cervix carcinoma cells upon high glucose cultivation, PCK2 suppression and not activation decreased TCA cycle flux (52). In that model PCK2 inhibition increased ROS formation upon treatment with high and low glucose media. The increase in ROS was connected to increased proline degradation by proline dehydrogenase, as this enzyme forms ROS as a by-product (52). In A549 lung cancer cells, treated for 48 hours with no glucose but 10% dialyzed serum, PCK2 expression did not alter $^{13}C_5$ incorporation into TCA cycle intermediates however abundances were normalized to high glucose conditions (43). In liver cancer cells, PCK1 overexpression reduced the abundance of TCA cycle intermediates because of cataplerosis independent of the glucose concentration. Increased cataplerosis resulted in enhanced ROS formation, an energy crisis and reduced cell viability (50). Contrary, in colon cancer cells, PCK1 cells silencing diminished $^{13}C_3$ lactic acid and $^{13}C_5$ glutamine incorporation into the TCA cycle (47,87).

In the liver and intestine of non-tumor bearing PCK1 knockout mice, the abundance of TCA cycle metabolites was enhanced as cataplerosis was decreased (88-91). Contrary to the findings shown here, in the liver from mice fed with a high fat diet, cataplerosis by PCK1 enhanced TCA cycle flux and mitochondrial respiration (91). Reduced TCA cycle flux and mitochondrial respiration were connected to a reduced NAD/NADH ratio in the knockdown liver (91).

All these studies show that the role of PCK1/PCK2 expression on the abundance of TCA cycle intermediates as well as on their interconversion is highly complex and tissue and context dependent and might be also connected to the cellular NADH/energy status. Potentially the effect of PCK1/PCK2 on the TCA cycle is dependent on its activity itself, which is varying between different tissues of origin and between altered nutritional states.

Although primarily considered as starting point for various biosynthetic pathways, TCA intermediates are also highly involved into cell signaling and influence gene expression. Acetyl CoA derived from citrate provides the acetyl groups for acetylation of histones and of proteins, one major post translational modification (81). If leucine residues of histones are acetylated, chromatin is less condensed and gene transcription is favored. Low levels of αKG regulate HIF1α stability as reduced levels of αKG impair prolyl hydrolase activity, which then cannot hydroxylate HIF anymore. Therefore, HIF is not ubiquitinylated and accumulates. Additionally, under normoxia, HIF is also stabilized by high levels of succinate and fumarate leading to a pseudohypoxic state (81). High succinate levels additionally lead to histone and DNA methylation. Whereas histone methylation is generally considered to induce gene expression, DNA methylation reduces transcription of respective DNA areas (81). Accumulation of high levels of fumarate also increase DNA hypermethylation. Fumarate can also cause succination, meaning that fumarate binds to and deactivates thiol protein residues. Succination of KEAP1 was discovered to lead to the accumulation of the antioxidative regulator NRF2 (81). Additionally, high fumarate levels induce succination of GSH, reduced GSH/GSSG levels and therefore ROS (81,92). These different signaling functions raise the question if the increased abundance of TCA cycle intermediates, found upon our experimental conditions by PCK2 silencing, cause alterations in gene expression and cellular signaling. Potentially, enhanced fumarate levels by PCK2 silencing, induced succination of GSH, which, combined with ROS originating from mitochondrial respiration, reduced the glutathione redox balance.

Beside the role of TCA cycle intermediates as starting point for variable anabolic pathways as nucleotide, amino acid and fatty acid synthesis, their signaling function and their regulatory effect on gene expression, the flux through the cycle plays a role for the redox homeostasis as thereby NADPH can be regained. The conversion of isocitrate to αKG by isocitrate dehydrogenase produces NADPH from $NADP^+$ but also synthesis of pyruvate from malate by malic enzyme eventually yields NADPH (13,31). NADPH production by flux through the cycle might be beneficial for maintaining the redox balance. However, we show, that enhancing the TCA cycle activity by PCK2 silencing but also by the exogeneous additions of DMM, leads to augmented mitochondrial respiration which subsequently decreased the redox potential. This finding is in line with a previous publication, which reports that ROS formation dose dependently increased through DMM addition in lung cancer cells (93).

4.3. Respiration and redox stress are increased by PCK2 silencing due to increased TCA cycle activity

Flux through the TCA cycle is connected to the production of reducing equivalents (NADH and $FADH_2$) which are used to create a proton motive force and subsequently produce ATP, during the process of oxidative phosphorylation. We found that mitochondrial respiration was enhanced by nutrient starvation, which is consistent with a previous report that shows that glucose starvation enhances respiration in a set of cancer cell lines (18). In high glucose medium, PCK2 expression enhanced oxygen consumption in melanoma, breast cancer, glioma and pancreatic neuroendocrine tumor cells (46,49,94,95) and PCK1 overexpression led to higher oxygen consumption in colon cancer cells (87). However, to the best of our knowledge, the effect of PCK1 or PCK2 expression on mitochondrial respiration upon nutrient deprivation was not assessed so far. Contrary to the previous findings in nutrient replete conditions (46,49,94,95) we discovered that PCK2 silencing led to increased mitochondrial respiration, whereas upon non-starvation treatment basal oxygen consumption was not altered by PCK2 silencing in our experimental setting. Of note we also found that upon starvation treatment the addition of DMM led to increased mitochondrial respiration which is consistent with a previous finding showing that malate accumulation, induced by silencing of ME2 was shown to induce enhanced OXPHOS (93).

We measured mitochondrial respiration upon the presence of lactate or pyruvate as a metabolic fuel. However, upon starvation, in the absence of lactate and pyruvate, we found that cells continue to respire and PCK2 silencing leads to a similar increase in mitochondrial respiration than if lactate is present. A comparable effect we also discovered when we added an inhibitor of fatty acid oxidation. It is surprising that despite glucose and serum starvation, cancer cells remain very flexible towards different metabolic substrates and they continue to respire, also in the absence of single fuels. Potentially, in the absence of lactate or fatty acid oxidation derived acetyl-CoA, cells utilize branched chain amino acids (leucine, isoleucine and valine) which can be taken up from the culture media and are available in the plasma (13).

As discussed before, we found that PCK2 silencing increases the abundance of TCA cycle metabolites, which was pronounced upon glucose and serum starvation. Consequently, mitochondrial respiration was enhanced by PCK2 silencing upon starvation treatment. The mitochondrial ETC is the major cause of ROS, due to electron leakage, which can be scavenged by antioxidant enzymes at the expense of NADPH or GSH (12,84). We discovered that the expression of a panel of antioxidant defense genes, namely *NFE2L2*, *SLC7A11*, *TXNRD1, GSR, GPX1* and *GPX4* were at least partly upregulated by treatment with starvation media pointing out a counteraction to a rise in ROS. Enhanced levels of *NFE2L2* and *SLC7A11* in starved cells have been previously reported (72). Many of the upregulated genes such as *GPX1*, *GPX4* and *TXNRD1* utilize GSH or NADPH as a co-factor (84). We found that the GSH/GSSG and subsequently the NADPH/$NADP^+$ ratio was reduced by PCK2 silencing upon starvation treatment. Surprisingly ROS levels were not increased by PCK2 silencing by our experimental setup, hinting that emerging ROS were continuously scavenged by antioxidative enzymes by using GSH and NADPH.

When we externally challenged the system through adding a GPX4 inhibitor, PCK2 silencing resulted in enhanced lipid peroxidation compared to control cells. Moreover, PCK2 silenced cells were more sensitive towards the addition of external H_2O_2 than control cells. Together, these data show that PCK2 expression allows the maintenance of the cellular antioxidant defense in starved lung cancer cells.

We found that the expression of SLC7A11 mRNA was partially upregulated upon PCK2 expression, however on a protein level no differences could be detected. Besides being regulated on a transcriptional level, SLC7A11 expression is also affected by post-translational modifications and by its binding partner SLCA3A2 (96). Additionally, SLC7A11 expression, which is upregulated upon glucose starvation (72), can lead to oxidative stress. Imported cystine needs to be reduced by NADPH to cysteine and therefore cells with high SLC7A11 expression and low PPP activity, as induced by glucose starvation, can run into a NADPH deprivation crisis, leading to cell death (96,97).

A balanced GSH/GSSG ratio is not only beneficial to avoid the accumulation of ROS but it also prevents S-gluathionylation of proteins. S-glutathionylation changes the protein function and might affect all proteins including signaling proteins such as protein kinase C or NF-κB (86). We discovered an increased expression of the GSH-dependent deglutathionylating enzymes sulfiredoxin or GLRX but not of GSTP, mediating glutathionylation upon treatment with starvation media. This might be connected to an increased rate of spontaneous protein-glutathionylation due to a reduced GSH/GSSG ratio.

Starved cancer cells upregulate the expression of antioxidant defense genes such as NRF2 or SLC7A11 as shown by us and others (72). This implies that nutrient deprivation might lead to enhanced levels of ROS. Previous reports showed that glucose starvation and extended nutrient deprivation induced by treatment with Hank's balanced salt solution (HBSS) activated ROS formation (72,98-100). In an *in vivo* model of glucose deprivation, ketogenic diet, mice fed with the low carbohydrate diet had a higher burden of lipid peroxidation in tumors upon radiation therapy, and the treatment efficiency was increased (101). Although the reasons for enhanced oxidative stress upon nutrient starvation treatment are not known so far, enhanced mitochondrial respiration combined with an impaired ability of antioxidant cofactors such as GSH or NADPH might play a role.

4.4. Colony forming cells show sensitivity towards oxidative stress and PCK2 silencing

In our study, we identified an important role of PCK2 mediated cataplerosis, which causes balancing of mitochondrial respiration and subsequently of ROS formation upon starvation treatment. PCK2 silencing did not induce ROS formation in confluent cells, but the GSH/GSSG ratio was clearly decreased, indicating an increased need to scavenge antioxidants. Proliferation and cell numbers were not affected by PCK2 silencing. However, upon loose plating conditions PCK2 silencing severely reduced the colony formation ability under starvation conditions. When inducing oxidative stress by blocking GSH de novo synthesis, we found that loosely plated, colony forming cells were affected dramatically whereas the effects on densely plated cells were minor. We concluded that sparsely plated, colony forming cells, are more sensitive towards additional oxidative stress. This is in line with a previous report showing that certain cell types have increased ROS burden upon loose plating densities (102).

We found that GSH and NAC, serving as precursor of GSH but also as direct antioxidant, not only rescued impaired colony formation caused by PCK2 but additionally also led to an increased colony formation potential upon starvation treatment in control cells. This suggests that upon starvation conditions colony forming cells are dependent on antioxidant systems. Addition of DMM, the analogue of the TCA cycle metabolite malate, mimicked the effect of PCK2 silencing. Additionally, also the induction of protein glutathionylation by diamide decreased colony formation. In summary, these data show that PCK2's role in balancing the redox levels supports cell survival and the colony forming ability of starved lung cancer cells. Phenotypic changes and the form of cell death or growth arrest of PCK2 silenced cells during the colony formation process has not been clarified and remains to be investigated.

In general, the colony formation model serves as an *in vitro* model to determine the survival of single cells throughout a period of metabolic stress followed by the ability to proliferate in full growth media thereafter. Although colony formation is not a direct *in vitro* model of metastases formation, abilities of colony forming cells are also required during metastases. A previous study in lung cancer patients, reported that PCK1/2 expression is enhanced in metastases in comparison to the primary tumor of lung cancer patients (39), which fits to our data showing that especially colony forming cells are in need of PCK2. To identify the role of PCK2 for

metastases of lung cancer cells future studies with more revelatory methods *in vitro* with and *in vivo* are warranted.

Apart from cell death, induced by a ROS imbalance, diminished colony formation might derive from alterations in cell signaling. In a previous study in glucose starved lung cancer cells, PCK2 has been shown to mediate the synthesis of glycerol phosphate for the phospholipid backbone. The addition of exogeneous phosphatidylethanolamine phospholipids partially rescued the impaired colony forming ability by PCK2 silencing (44). Interestingly, phosphatidylethanolamine is easily peroxidated, particularly when containing polyunsaturated fatty acids (103). Therefore, the synthesis and turnover of PE, facilitated by PCK2 expression, combined with TCA activity limiting effects of PCK2 described in this study synergize to balance ROS induced alterations under nutrient starvation.

4.5. Limitations

Most experiments in this study except of the colony formation and some cell counting assays, have been conducted with a treatment time of 24 hours, reflecting phenotypic changes. However, especially for ROS detection measurements, it would be interesting to assess longer treatment periods as this might influence PCK2 silenced cells to a more severe extent than after short treatment durations as GSH and NADPH pools are potentially depleted.

When colony formation was assessed, two different siRNA pools were used for the A549 cell line and in H23 cells a shRNA and a siRNA approach were utilized. However, to confirm the specificity of the silencing, it was tried to additionally include colony formation experiments with the PCK2 re-expression system in this study. In preliminary experiments it was discovered that colony formation was severely impaired when utilizing the plasmid based PCK2 rescue system by both, the control plasmid and the PCK2 plasmid, especially in the context of starvation. Enhanced cell death due to the plasmid transfection in combination with a low seeding density might be the cause. Stable PCK2 overexpression potentially might overcome this problem, but we were not able to obtain stably PCK2 re-expressing clones after antibiotics selection, possibly due to adverse effects of chronic PCK2 overexpression in the cultured cells.

The present study sheds light into the cataplerotic role of PCK2 in starved lung cancer cells *in vitro*. *In vitro* cancer cell cultures provide valuable information about cellular adaptations, however *in vivo* models are warranted to determine the relevance of the findings. Two NSCLC xenograft studies showed that PCK2 knockdown by shRNA led to almost no tumor growth (43,44), precluding detailed analyses of the mechanism involved. An inducible approach or a specific PCK2 inhibitor could circumvent this problem. Unfortunately, silencing was not sufficient in preliminary experiments using an IPTG-inducible shRNA system *in vivo*.

4.6. Conclusion and outlook

In summary, these results reveal that cataplerosis mediated by PCK2 directly decreases the abundance of TCA cycle intermediates and their interconversion, reduces starvation-induced mitochondrial respiration and depletes cellular GSH in starved lung cancer cells. This equilibrium, however, is critical for the cellular colony forming potential especially upon starvation treatment and has a protective role scavenging exogenous ROS. A model for PCK2's cataplerotic role for limiting respiration and maintaining the glutathione redox balance in cancer cells is proposed in Figure 17.

Although metabolic pathways mediated by PCK1 and PCK2 are highly investigated in the past years, until recently nothing was known about non-canonical, so-called moonlighting, functions. Recently it has been shown that phosphorylated PCK1 can translocate to the ER and phosphorylate an inhibitor of sterol regulatory element-binding proteins (SREBP) which then dissociates. This leads to SREBP mediated lipogenesis induced by PCK1 phosphorylation (104). For PCK2, no non-canonical functions are known so far. However, we identified a role of PCK2 in regulating TCA cycle abundance and interconversion also in non-starved cancer cells, conditions with low levels of gluconeogenesis and therefore cataplerosis. It is possible that also PCK2 has a certain moonlighting regulatory role which might be investigated in future studies.

How cancer cells regulate TCA cycle activity, mitochondrial respiration and the redox balance, especially under nutrient deprivation is still poorly understood. Moreover, the contribution of intratumoral gluconeogenesis as opposed to glycolysis to tumor metabolism, e.g. in poorly

vascularized tumors or tumor regions is not clear. The present study sheds light on the role of PCK2 as a regulator of mitochondrial metabolism and respiration under starvation conditions and helps in understanding the mechanisms of cancer cell adaptation to their harsh microenvironment. As a conclusion, PCK2 inhibition potentially in combination with a ketogenic diet to induce glucose starvation, might represent a novel therapeutic approach in the future to avoid metabolic adaptation and to distort the redox equilibrium in lung cancer cells. Recently, novel inhibitors of PCK2 were developed and their inhibitory potential as well as their tolerance in mice were investigated (105).

5. References

(1) Bluemel G, Planque M, Madreiter-Sokolowski CT, Haitzmann T, Hrzenjak A, Graier WF, et al. PCK2 opposes mitochondrial respiration and maintains the redox balance in starved lung cancer cells. Free Radic Biol Med; 2021; 176:34-45.

(2) Dela Cruz CS, Tanoue LT, Matthay RA. Lung cancer: epidemiology, etiology, and prevention. Clin Chest Med; 2011; 32(4):605-644.

(3) Ramalingam SS, Owonikoko TK, Khuri FR. Lung cancer: New biological insights and recent therapeutic advances. CA Cancer J Clin; 2011; 61(2):91-112.

(4) Malhotra J, Malvezzi M, Negri E, La Vecchia C, Boffetta P. Risk factors for lung cancer worldwide. Eur Respir J; 2016; 48(3):889-902.

(5) Popper HH. Progression and metastasis of lung cancer. Cancer Metastasis Rev; 2016; 35(1):75-91.

(6) Polanski J, Jankowska-Polanska B, Rosinczuk J, Chabowski M, Szymanska-Chabowska A. Quality of life of patients with lung cancer. OncoTargets and therapy; 2016; 02/29;9:1023-1028.

(7) Duma N, Santana-Davila R, Molina JR. Non-Small Cell Lung Cancer: Epidemiology, Screening, Diagnosis, and Treatment. Mayo Clin Proc; 2019; 94(8):1623-1640.

(8) Pao W, Hutchinson KE. Chipping away at the lung cancer genome. Nat Med; 2012;18(3):349-351.

(9) Onoi K, Chihara Y, Uchino J, Shimamoto T, Morimoto Y, Iwasaku M, et al. Immune Checkpoint Inhibitors for Lung Cancer Treatment: A Review. Journal of clinical medicine; 2020; 05/06;9(5):1362.

(10) Majem B, Nadal E, Muñoz-Pinedo C. Exploiting metabolic vulnerabilities of Non small cell lung carcinoma. Semin Cell Dev Biol; 2020; 98:54-62.

(11) Vander Heiden MG, Cantley LC, Thompson CB. Understanding the Warburg effect: the metabolic requirements of cell proliferation. Science; 2009; 05/22;324(1095-9203; 0036-8075; 5930):1029-1033.

(12) Chandel N. Navigating Metabolism. 1st ed. Cold Spring Harbor, NY: Cold Spring Harbor Laboratory Press; 2015.

(13) DeBerardinis RJ, Chandel NS. Fundamentals of cancer metabolism. Sci Adv; 2016; 27;2(5):e1600200.

(14) Hanahan D, Weinberg RA. Hallmarks of cancer: the next generation. Cell; 2011; 144(5):646-674.

(15) Warburg O, Wind F, Negelein E. The Metabolism of Tumors in the Body. J Gen Physiol; 1927; 8(6):519-530.

(16) Fletcher JW, Djulbegovic B, Soares HP, Siegel BA, Lowe VJ, Lyman GH, et al. Recommendations on the use of 18F-FDG PET in oncology. J Nucl Med; 2008; 49(3):480-508.

(17) Boroughs LK, DeBerardinis RJ. Metabolic pathways promoting cancer cell survival and growth. Nat Cell Biol; 2015; 17(4):351-359.

(18) Birsoy K, Possemato R, Lorbeer FK, Bayraktar EC, Thiru P, Yucel B, et al. Metabolic determinants of cancer cell sensitivity to glucose limitation and biguanides. Nature; 2014; 508(7494):108-112.

(19) Pavlova NN, Thompson CB. The Emerging Hallmarks of Cancer Metabolism. Cell Metab; 2016; 23(1):27-47.

(20) Romero-Garcia S, Moreno-Altamirano M, Prado-Garcia H, Sánchez-García FJ. Lactate Contribution to the Tumor Microenvironment: Mechanisms, Effects on Immune Cells and Therapeutic Relevance. Frontiers in immunology; 2016; 02/16;7:52-52.

(21) Chiche J, Brahimi-Horn M, Pouysségur J. Tumour hypoxia induces a metabolic shift causing acidosis: a common feature in cancer. J Cell Mol Med; 2010; 04;14(4):771-794.

(22) Zhang D, Tang Z, Huang H, Zhou G, Cui C, Weng Y, et al. Metabolic regulation of gene expression by histone lactylation. Nature; 2019; 10;574(7779):575-580.

(23) Martin JD, Fukumura D, Duda DG, Boucher Y, Jain RK. Reengineering the Tumor Microenvironment to Alleviate Hypoxia and Overcome Cancer Heterogeneity. Cold Spring Harb Perspect Med; 2016; 6(12):10.1101/cshperspect.a027094.

(24) Vaupel P. Tumor microenvironmental physiology and its implications for radiation oncology. Semin Radiat Oncol; 2004; 14(3):198-206.

(25) Sullivan MR, Danai LV, Lewis CA, Chan SH, Gui DY, Kunchok T, et al. Quantification of microenvironmental metabolites in murine cancers reveals determinants of tumor nutrient availability. Elife; 2019; 8:e44235.

(26) Cairns RA, Harris IS, Mak TW. Regulation of cancer cell metabolism. Nat Rev Cancer; 2011; 11(2):85-95.

(27) Lehuede C, Dupuy F, Rabinovitch R, Jones RG, Siegel PM. Metabolic Plasticity as a Determinant of Tumor Growth and Metastasis. Cancer Res; 2016;76(18):5201-5208.

(28) Fendt SM, Frezza C, Erez A. Targeting Metabolic Plasticity and Flexibility Dynamics for Cancer Therapy. Cancer Discov; 2020; 10(12):1797-1807.

(29) Grasmann G, Mondal A, Leithner K. Flexibility and Adaptation of Cancer Cells in a Heterogenous Metabolic Microenvironment. International journal of molecular sciences; 2021; 02/02;22(3):1476.

(30) Hosios AM, Hecht VC, Danai LV, Johnson MO, Rathmell JC, Steinhauser ML, et al. Amino Acids Rather than Glucose Account for the Majority of Cell Mass in Proliferating Mammalian Cells. Dev Cell; 2016; 36(5):540-549.

(31) DeBerardinis RJ, Cheng T. Q's next: the diverse functions of glutamine in metabolism, cell biology and cancer. Oncogene; 2010; 29(3):313-324.

(32) Kallinowski F, Runkel S, Fortmeyer HP, Förster H, Vaupel P. L-glutamine: a major substrate for tumor cells *in vivo*? J Cancer Res Clin Oncol; 1987; 113(3):209-215.

(33) Kennedy KM, Scarbrough PM, Ribeiro A, Richardson R, Yuan H, Sonveaux P, et al. Catabolism of exogenous lactate reveals it as a legitimate metabolic substrate in breast cancer. PLoS One; 2013; 8(9):e75154.

(34) Sonveaux P, Vegran F, Schroeder T, Wergin MC, Verrax J, Rabbani ZN, et al. Targeting lactate-fueled respiration selectively kills hypoxic tumor cells in mice. J Clin Invest; 2008; 12;118(0021-9738; 0021-9738; 12):3930-3942.

(35) Vander Heiden MG, DeBerardinis RJ. Understanding the Intersections between Metabolism and Cancer Biology. Cell 2017; 168(4):657-669.

(36) Owen OE, Kalhan SC, Hanson RW. The key role of anaplerosis and cataplerosis for citric acid cycle function. J Biol Chem; 2002; 277(34):30409-30412.

(37) Grasmann G, Smolle E, Olschewski H, Leithner K. Gluconeogenesis in cancer cells - Repurposing of a starvation-induced metabolic pathway? Biochim Biophys Acta Rev Cancer; 2019; 1872(1):24-36.

(38) Stark R, Kibbey RG. The mitochondrial isoform of phosphoenolpyruvate carboxykinase (PEPCK-M) and glucose homeostasis: has it been overlooked? Biochim Biophys Acta; 2014; 1840(4):1313-1330.

(39) Smolle E, Leko P, Stacher-Priehse E, Brcic L, El-Heliebi A, Hofmann L, et al. Distribution and prognostic significance of gluconeogenesis and glycolysis in lung cancer. Mol Oncol; 2020; 11:2853-2867.

(40) TeSlaa T, Bartman CR, Jankowski CSR, Zhang Z, Xu X, Xing X, et al. The Source of Glycolytic Intermediates in Mammalian Tissues. Cell Metab; 2021; 33:367-378.e5.

(41) Leithner K, Hrzenjak A, Trotzmuller M, Moustafa T, Kofeler HC, Wohlkoenig C, et al. PCK2 activation mediates an adaptive response to glucose depletion in lung cancer. Oncogene; 2015; 34(8):1044-1050.

(42) Mendez-Lucas A, Hyrossova P, Novellasdemunt L, Vinals F, Perales JC. Mitochondrial Phosphoenolpyruvate Carboxykinase (PEPCK-M) Is a Pro-survival, Endoplasmic Reticulum (ER) Stress Response Gene Involved in Tumor Cell Adaptation to Nutrient Availability. J Biol Chem; 2014; 289(32):22090-22102.

(43) Vincent EE, Sergushichev A, Griss T, Gingras MC, Samborska B, Ntimbane T, et al. Mitochondrial Phosphoenolpyruvate Carboxykinase Regulates Metabolic Adaptation and Enables Glucose-Independent Tumor Growth. Mol Cell; 2015; 60(2):195-207.

(44) Leithner K, Triebl A, Trotzmuller M, Hinteregger B, Leko P, Wieser BI, et al. The glycerol backbone of phospholipids derives from noncarbohydrate precursors in starved lung cancer cells. Proc Natl Acad Sci U S A; 2018; 115(24):6225-6230.

(45) Zhao J, Li J, Fan TWM, Hou SX. Glycolytic reprogramming through PCK2 regulates tumor initiation of prostate cancer cells. Oncotarget; 2017; 8(48):83602-83618.

(46) Chu PY, Jiang SS, Shan YS, Hung WC, Chen MH, Lin HY, et al. Mitochondrial phosphoenolpyruvate carboxykinase (PEPCK-M) regulates the cell metabolism of pancreatic neuroendocrine tumors (pNET) and de-sensitizes pNET to mTOR inhibitors. Oncotarget; 2017; 8(61):103613-103625.

(47) Montal ED, Dewi R, Bhalla K, Ou L, Hwang BJ, Ropell AE, et al. PEPCK Coordinates the Regulation of Central Carbon Metabolism to Promote Cancer Cell Growth. Mol Cell; 2015; 60(4):571-583.

(48) Li Y, Luo S, Ma R, Liu J, Xu P, Zhang H, et al. Upregulation of cytosolic phosphoenolpyruvate carboxykinase is a critical metabolic event in melanoma cells that repopulate tumors. Cancer Res; 2015; 75(7):1191-1196.

(49) Luo S, Li Y, Ma R, Liu J, Xu P, Zhang H, et al. Downregulation of PCK2 remodels tricarboxylic acid cycle in tumor-repopulating cells of melanoma. Oncogene; 2017; 36(25):3609-3617.

(50) Liu MX, Jin L, Sun SJ, Liu P, Feng X, Cheng ZL, et al. Metabolic reprogramming by PCK1 promotes TCA cataplerosis, oxidative stress and apoptosis in liver cancer cells and suppresses hepatocellular carcinoma. Oncogene; 2018; 37(12):1637-1653.

(51) Keshet R, Lee JS, Adler L, Iraqi M, Ariav Y, Lim LQJ, et al. Targeting purine synthesis in ASS1-expressing tumors enhances the response to immune checkpoint inhibitors. Nat Cancer; 2020; 1,894–908.

(52) Hyroššová P, Aragó M, Moreno-Felici J, Fu X, Mendez-Lucas A, García-Rovés PM, et al. PEPCK-M recoups tumor cell anabolic potential in a PKC-ζ-dependent manner. Cancer Metab; 2021;9(1):1-020-00236-3.

(53) Chakravarty K, Cassuto H, Reshef L, Hanson RW. Factors that control the tissue-specific transcription of the gene for phosphoenolpyruvate carboxykinase-C. Crit Rev Biochem Mol Biol; 2005; 40(3):129-154.

(54) Carroll PA, Diolaiti D, McFerrin L, Gu H, Djukovic D, Du J, et al. Deregulated Myc requires MondoA/Mlx for metabolic reprogramming and tumorigenesis. Cancer Cell; 2015; 27(2):271-285.

(55) Sun Y, Gao J, Jing Z, Zhao Y, Sun Y, Zhao X. PURα Promotes the Transcriptional Activation of PCK2 in Oesophageal Squamous Cell Carcinoma Cells. Genes (Basel) 2020; 11(11):1301. doi: 10.3390/genes11111301.

(56) Bian XL, Chen HZ, Yang PB, Li YP, Zhang FN, Zhang JY, et al. Nur77 suppresses hepatocellular carcinoma via switching glucose metabolism toward gluconeogenesis through attenuating phosphoenolpyruvate carboxykinase sumoylation. Nat Commun; 2017; 8:14420.

(57) Jiang W, Wang S, Xiao M, Lin Y, Zhou L, Lei Q, et al. Acetylation regulates gluconeogenesis by promoting PEPCK1 degradation via recruiting the UBR5 ubiquitin ligase. Mol Cell; 2011; 43(1):33-44.

(58) Goldstein I, Yizhak K, Madar S, Goldfinger N, Ruppin E, Rotter V. P53 Promotes the Expression of Gluconeogenesis-Related Genes and Enhances Hepatic Glucose Production. Cancer Metab; 2013; 1(1):9-3002-1-9.

(59) Zhang P, Tu B, Wang H, Cao Z, Tang M, Zhang C, et al. Tumor suppressor p53 cooperates with SIRT6 to regulate gluconeogenesis by promoting FoxO1 nuclear exclusion. Proc Natl Acad Sci U S A; 2014; 111(29):10684-10689.

(60) Khan MW, Biswas D, Ghosh M, Mandloi S, Chakrabarti S, Chakrabarti P. mTORC2 controls cancer cell survival by modulating gluconeogenesis. Cell Death Discov; 2015; 1:15016.

(61) Tang K, Yu Y, Zhu L, Xu P, Chen J, Ma J, et al. Hypoxia-reprogrammed tricarboxylic acid cycle promotes the growth of human breast tumorigenic cells. Oncogene; 2019; 38(44):6970-6984.

(62) Yoboue ED, Sitia R, Simmen T. Redox crosstalk at endoplasmic reticulum (ER) membrane contact sites (MCS) uses toxic waste to deliver messages. Cell death & disease; 2018; 02/28;9(3):331-331.

(63) Harris IS, DeNicola GM. The Complex Interplay between Antioxidants and ROS in Cancer. Trends Cell Biol; 2020; 30(6):440-451.

(64) Baffy G. Mitochondrial uncoupling in cancer cells: Liabilities and opportunities. Biochim Biophys Acta Bioenerg; 2017; 1858(8):655-664.

(65) Sullivan LB, Chandel NS. Mitochondrial reactive oxygen species and cancer. Cancer Metab 2014; 2:17-3002-2-17. eCollection 2014.

(66) Yang WS, SriRamaratnam R, Welsch ME, Shimada K, Skouta R, Viswanathan VS, et al. Regulation of Ferroptotic Cancer Cell Death by GPX4. Cell; 2014; 01/16; 2020/09;156(1):317-331.

(67) Sasaki H, Sato H, Kuriyama-Matsumura K, Sato K, Maebara K, Wang H, et al. Electrophile response element-mediated induction of the cystine/glutamate exchange transporter gene expression. J Biol Chem; 2002; 277(47):44765-44771.

(68) Bansal A, Simon MC. Glutathione metabolism in cancer progression and treatment resistance. J Cell Biol; 2018; 217(7):2291-2298.

(69) Baffy G, Derdak Z, Robson SC. Mitochondrial recoupling: a novel therapeutic strategy for cancer? Br J Cancer; 2011; 105(4):469-474.

(70) Brenner C, Subramaniam K, Pertuiset C, Pervaiz S. Adenine nucleotide translocase family: four isoforms for apoptosis modulation in cancer. Oncogene; 2011; 02/01;30(8):883-895.

(71) Patra KC, Hay N. (2014) The pentose phosphate pathway and cancer Trends in Biochemical Sciences; 39(8):347-354

(72) Koppula P, Zhang Y, Shi J, Li W, Gan B. The glutamate/cystine antiporter SLC7A11/xCT enhances cancer cell dependency on glucose by exporting glutamate. J Biol Chem; 2017; 292(34):14240-14249.

(73) Ahmad IM, Aykin-Burns N, Sim JE, Walsh SA, Higashikubo R, Buettner GR, et al. Mitochondrial O2*- and H2O2 mediate glucose deprivation-induced stress in human cancer cells. J Biol Chem; 2005; 280(6):4254-4263.

(74) Krebs HA. Rate control of the tricarboxylic acid cycle. Adv Enzyme Regul; 1970; 8:335-353.

(75) Lorendeau D, Rinaldi G, Boon R, Spincemaille P, Metzger K, Jager C, et al. Dual loss of succinate dehydrogenase (SDH) and complex I activity is necessary to recapitulate the metabolic phenotype of SDH mutant tumors. Metab Eng; 2017; 43:187-197.

(76) Millard P, Delepine B, Guionnet M, Heuillet M, Bellvert F, Letisse F. IsoCor: isotope correction for high-resolution MS labeling experiments. Bioinformatics; 2019; 35(21):4484-4487.

(77) Kampen KR, Fancello L, Girardi T, Rinaldi G, Planque M, Sulima SO, et al. Translatome analysis reveals altered serine and glycine metabolism in T-cell acute lymphoblastic leukemia cells. Nature Communications; 2019; 10:2542.

(78) Valente AJ, Maddalena LA, Robb EL, Moradi F, Stuart JA. A simple ImageJ macro tool for analyzing mitochondrial network morphology in mammalian cell culture. Acta Histochem; 2017; 119(3):315-326.

(79) Guzman C, Bagga M, Kaur A, Westermarck J, Abankwa D. ColonyArea: an ImageJ plugin to automatically quantify colony formation in clonogenic assays. PLoS One; 2014; 9(3):e92444.

(80) Yang C, Ko B, Hensley CT, Jiang L, Wasti AT, Kim J, et al. Glutamine oxidation maintains the TCA cycle and cell survival during impaired mitochondrial pyruvate transport. Mol Cell; 2014; 11/06;56(3):414-424.

(81) Martínez-Reyes I, Chandel NS. Mitochondrial TCA cycle metabolites control physiology and disease. Nature Communications; 2020; 01/03;11(1):102.

(82) Rambold AS, Kostelecky B, Elia N, Lippincott-Schwartz J. Tubular network formation protects mitochondria from autophagosomal degradation during nutrient starvation. Proc Natl Acad Sci U S A; 2011; 108(25):10190-10195.

(83) Mishra P, Chan DC. Metabolic regulation of mitochondrial dynamics. J Cell Biol; 2016; 212(4):379-387.

(84) Reczek CR, Chandel NS. ROS-dependent signal transduction. Curr Opin Cell Biol; 2015; 33:8-13.

(85) Chouchani ET, Pell VR, Gaude E, Aksentijevic D, Sundier SY, Robb EL, et al. Ischaemic accumulation of succinate controls reperfusion injury through mitochondrial ROS. Nature; 2014; 515(7527):431-435.

(86) Mieyal JJ, Gallogly MM, Qanungo S, Sabens EA, Shelton MD. Molecular mechanisms and clinical implications of reversible protein S-glutathionylation. Antioxid Redox Signal; 2008; 10(11):1941-1988.

(87) Montal ED, Bhalla K, Dewi RE, Ruiz CF, Haley JA, Ropell AE, et al. Inhibition of phosphoenolpyruvate carboxykinase blocks lactate utilization and impairs tumor growth in colorectal cancer. Cancer Metab; 2019; 7:8-019-0199-6. eCollection 2019.

(88) Burgess SC, Hausler N, Merritt M, Jeffrey FM, Storey C, Milde A, et al. Impaired tricarboxylic acid cycle activity in mouse livers lacking cytosolic phosphoenolpyruvate carboxykinase. J Biol Chem; 2004; 279(47):48941-48949.

(89) Potts A, Uchida A, Deja S, Berglund ED, Kucejova B, Duarte JAG, et al. Cytosolic Phosphoenolpyruvate Carboxykinase as a Cataplerotic Pathway in the Small Intestine. Am J Physiol Gastrointest Liver Physiol; 2018; 315(2):G249-G258.

(90) She P, Shiota M, Shelton KD, Chalkley R, Postic C, Magnuson MA. Phosphoenolpyruvate carboxykinase is necessary for the integration of hepatic energy metabolism. Mol Cell Biol; 2000; 20(17):6508-6517.

(91) Satapati S, Kucejova B, Duarte JA, Fletcher JA, Reynolds L, Sunny NE, et al. Mitochondrial metabolism mediates oxidative stress and inflammation in fatty liver. J Clin Invest; 2015; 125(12):4447-4462.

(92) Zheng L, Cardaci S, Jerby L, MacKenzie ED, Sciacovelli M, Johnson TI, et al. Fumarate induces redox-dependent senescence by modifying glutathione metabolism. Nat Commun; 2015; 6:6001.

(93) Ren JG, Seth P, Clish CB, Lorkiewicz PK, Higashi RM, Lane AN, et al. Knockdown of malic enzyme 2 suppresses lung tumor growth, induces differentiation and impacts PI3K/AKT signaling. Sci Rep; 2014; 4:5414.

(94) Lin J, Wu S, Ye S, Papa APD, Yang J, Huang S, et al. Oridonin interrupts cellular bioenergetics to suppress glioma cell growth by down-regulating PCK2. Phytother Res; 2021.

(95) Chao C, Wang C, Wang C, Chen T, Hsu H, Huang H, et al. Mutant p53 Attenuates Oxidative Phosphorylation and Facilitates Cancer Stemness through Downregulating miR-200c–PCK2 Axis in Basal-Like Breast Cancer. Mol Cancer Res; 2021; 07/26.

(96) Koppula P, Zhang Y, Zhuang L, Gan B. Amino acid transporter SLC7A11/xCT at the crossroads of regulating redox homeostasis and nutrient dependency of cancer. Cancer Commun (Lond); 2018; 38(1):12-018-0288-x.

(97) Liu X, Olszewski K, Zhang Y, Lim EW, Shi J, Zhang X, et al. Cystine transporter regulation of pentose phosphate pathway dependency and disulfide stress exposes a targetable metabolic vulnerability in cancer. Nat Cell Biol; 2020; 04/01;22(4):476-486.

(98) Jelluma N, Yang X, Stokoe D, Evan GI, Dansen TB, Haas-Kogan DA. Glucose withdrawal induces oxidative stress followed by apoptosis in glioblastoma cells but not in normal human astrocytes. Mol Cancer Res; 2006; 4(5):319-330.

(99) Owada S, Shimoda Y, Tsuchihara K, Esumi H. Critical role of H2O2 generated by NOX4 during cellular response under glucose deprivation. PLoS One; 2013; 8(3):e56628.

(100) De Saedeleer CJ, Porporato PE, Copetti T, Pérez-Escuredo J, Payen VL, Brisson L, et al. Glucose deprivation increases monocarboxylate transporter 1 (MCT1) expression and MCT1-dependent tumor cell migration. Oncogene; 2014; 33(31):4060-4068.

(101) Allen BG, Bhatia SK, Buatti JM, Brandt KE, Lindholm KE, Button AM, et al. Ketogenic diets enhance oxidative stress and radio-chemo-therapy responses in lung cancer xenografts. Clin Cancer Res; 2013; 19(14):3905-3913.

(102) Pani G, Colavitti R, Bedogni B, Anzevino R, Borrello S, Galeotti T. Determination of intracellular reactive oxygen species as function of cell density. Methods Enzymol; 2002; 352:91-100.

(103) Kagan VE, Mao G, Qu F, Angeli JP, Doll S, Croix CS, et al. Oxidized arachidonic and adrenic PEs navigate cells to ferroptosis. Nat Chem Biol; 2017; 13(1):81-90.

(104) Xu D, Wang Z, Xia Y, Shao F, Xia W, Wei Y, et al. The gluconeogenic enzyme PCK1 phosphorylates INSIG1/2 for lipogenesis. Nature; 2020; 580(7804):530-535.

(105) Arago M, Moreno-Felici J, Abas S, Rodriguez-Arevalo S, Hyrossova P, Figueras A, et al. Pharmacology and preclinical validation of a novel anticancer compound targeting PEPCK-M. Biomed Pharmacother; 2020;121:109601.